The mechanism of astringency sensation induced by green tea catechins.

緑茶カテキンが引き起こす渋味感覚の機構の解明

A Doctoral Thesis

Submitted to Graduate School of Bioscience

Nagahama Institute of Bio-science and Technology

Mako Kurogi

March 2014

TABLE OF CONTENTS

Chapter Ⅰ.
Green tea polyphenol epigallocatechin gallate activates TRPA1 in an intestinal enteroendocrine cell line, STC-1

Chapter Ⅱ .
Auto-oxidation products of epigallocatechin gallate activate TRPA1 and TRPV1 in sensory neurons.

General Abstract

For 5 basic taste stimuli including sweet, umami, bitter, salty, and sour, tastants are detected mainly by taste receptor cells in taste buds on the tongue.   In addition to 5 basic taste stimuli, the pungent stimulation of hot peppers and the astringent stimulation of major catechin of green tea EGCG are also recognized in the mouth. This pungent taste is mainly mediated by TRPV1 receptors, which can be activated by capsaicin from pepper and are expressed in sensory neurons in the oral cavity.   TRPV1 receptors are activated by a wide range of molecules including alcohols, terpenoids, aldehyde, and vanilloids such as capsaicin.

The sensation mechanism of astringency taste activated with a major catechin of green tea, EGCG has not been well understood, and it is not known which molecule functions as an EGCG sensor on the tongue. Here, I first found that the mouse intestinal endocrine cell line STC-1 responds to EGCG by elevating intracellular Ca^{2+} ($[Ca^{2+}]_i$) levels.   I further found that HEK293T cells transfected with the mouse TRPA1 cDNA showed $[Ca^{2+}]_i$ response upon application of EGCG, and that their response properties were similar to those observed in STC-1 cells.   These results indicated that EGCG activates TRPA1 in intestinal STC-1 cells (Kurogi et al., 2012).   I further found that TRPV1 is also activated by EGCG.

It is known that TRPA1 and TRPV1 channels are expressed in sensory neurons on the tongue.   It has been considered that green tea catechins pre-incubated for longer period taste more astringent.   Next, I examined how TRPA1 and TRPV1 are activated by EGCG in the course of auto-oxidation process.   Quite interestingly, freshly prepared EGCG without pre-incubation could not activate these TRP channels, but that only the incubated EGCG could activate them.   The presence of ascorbic acid largely inhibited the pre-incubation effect on EGCG.   These results strongly suggested that only

oxidative products of EGCG act as a ligand for the astringent sensors of TRPA1 and TRPV1. Then, I found that theasinensin A (TS-A) is one of the astringent sensor activators, which are formed during the auto-oxidation of EGCG. Furthermore, neurons of dorsal root ganglion (DRG) were isolated from mice and cultured, then, I examined their sensitivity to pre-incubated EGCG and to TS-A. I demonstrated that the oxidized EGCG and TS-A can directly activate TRPV1 and TRPA1 channels in DRG sensory neurons. These studies strongly suggested that the sense of astringency at green tea catechins such as TS-A may be caused by activating TRPV1 and TRPA1 channels with oxidized catechins such as TS-A in sensory neurons in the tongue and the mouth.

General Introduction

Humans have a multitude of senses. The purpose of the major senses is to detect and discriminate among signals coming from our environment. These signals carry information necessary for us to support our vital functions, such as taste and smell in eating, as well as functions used in communicating with others and in our work, such as sight, touch, and hearing. In addition to the traditional five senses, other senses of which we are not aware are at work within our bodies, such as the sense of balance and the sense of muscle effort, called kinesthesia, and many senses involved in detecting chemical changes in the blood and other tissues.

Animals, including humans, depend on the chemical senses to help identify nourishment, noxious substances, or the suitability of a potential mate. It is well known that gustation and olfaction have a similar task of the detection of environmental chemicals. The senses of gustation (taste), olfaction (smell) and chemesthetic fall under the category of chemical senses. Specialized cells act as receptors for certain chemical compounds. As these compounds react with the receptors, an impulse is sent to the brain and is registered as a certain taste or smell. The receptors they contain are sensitive to the molecules in the food we eat, along with the air we breathe. The sense of taste is transduced by taste buds and is conveyed via three of the twelve cranial nerves. Cranial nerve VII, the facial nerve, carries taste sensations from the anterior two thirds of the tongue (excluding the circumvallate papillae) and soft palate. Cranial nerve IX the glossopharyngeal nerve carries taste sensations from the posterior one third of the tongue (including the circumvallate papillae). Also a branch of the vague nerve carries some taste sensations from the back of the oral cavity (i.e. pharynx and epiglottis). Information from these cranial nerves is processed by the gustatory system. Though there are small differences in sensation, which can be measured with highly

specific, all taste buds can respond to all types of basic taste. Sensitivity to all basic tastes is distributed across the whole tongue and indeed to other regions of the mouth where there are taste buds (epiglottis, soft palate). Olfaction is the sense of smell. In humans the sense of Smell is received in nasopharynx. Airborne molecules go into solution on moist epithelial surface of nasal passage. An olfactory receptors neuron sends an impulse via Cranial nerve I the olfactory nerve. Although 80-90% of what we think is "taste" actually is due to smell. In addition to the classical senses of taste and smell, anatomically separate systems in the mouth and nose provide additional sensory input from chemical stimulation. Various tasteless and odorless compounds, such as carbon dioxide and capsaicin, are potent chemical stimuli and important flavor compounds in foods and beverages. Such stimuli are often classified as trigeminal because they are capable of stimulating nerve endings in the nose, mouth, and eyes that are subserved by branches of the fifth cranial nerves (the trigeminals). These nerves carry signals for pain, touch, and temperature stimulation, and are generally associated with painful or irritating chemical stimuli, hot pepper and polyphenol being a good example. It has been considered that these chemical sensations may include pungent and astringent tastes.

Astringency is a sensory attribute that is described as a drying-out, roughening, and puckery sensation felt in the mouth. Foods that are often astringent include red wine, green and black teas, soy-based foods, and certain fruits, especially when they're not yet ripe. In these foods, astringency is caused by the polyphenolic compounds they contain. Polyphenols are the most common cause of astringency in foods, though acids, metal salts such as alum, and alcohols are known to also cause astringency (Green, 1993). However, the mechanism of astringency is not fully understood. It is known that one of the best characterized groups is the salivary PRPs, which form 70 % of the protein in

saliva. They appear to have several functions, but the most likely function of the proline-rich tandemly repeated section (which forms by far the largest part of the protein) is to bind plant polyphenols present in the diet and to reduce their harmful effects by forming precipitates (Mehansho et al., 1987; Murray et al., 1994). One theory for the astringent taste is that precipitation of PRPs from saliva reduces its ability of lubricate, and this loss of lubricity is perceived (Clifford, 1997). A second theory is that the sensation is caused by a direct effect of astringents on the oral surface and that PRPs play a protective role and reduce astringency by binding the astringent compounds (Horne et al., 2002). By electrophysiological recordings, it was demonstrated that chorda tympani nerve directly responses to astringent compounds in rodents (Schiffman et al., 1992). Therefore, it is possible that an unidentified protein may function as a receptor for astringency on sensory neuron of the tongue, and those PRPs may have inhibitory function for astringency.

Here, I investigated whether intestinal STC-1 cells, which can be activated with five basic tastants, may be also able to respond to the astringent compound of green tea, EGCG. Then, I found that STC-1 cells can respond to EGCG through activating TRPA1 channels. At the same time, I also found that another TRP channel, TRPV1 is activated with EGCG (Chapter Ⅰ).

Next, I studied how TRPA1 and TRPV1 were activated by EGCG in the course of auto-oxidation process, because it is known that green tea incubated for longer period tastes more astringent. Surprisingly, I found that freshly prepare EGCG could not activate these TRP channels, but that only the incubated EGCG could activate them. Then, finally, I found that theasinensin A is one of the TRP channel activators, which are formed during the auto-oxidation of EGCG and that this compound really directly activates sensory neurons through TRPA1 and TRPV1 channels (Chapter Ⅱ). Therefore,

I demonstrated that TRPV1 and TRPA1 channels may function as a receptor for astringency on sensory neurons of the tongue.

Chapter Ⅰ.

Green tea polyphenol epigallocatechin gallate activates TRPA1 in an intestinal enteroendocrine cell line, STC-1

Abstract

A characteristic astringent taste is elicited by polyphenols. Among the polyphenols, catechins and their polymers are the most abundant polyphenols in wine and tea. A typical green tea polyphenol is epigallocatechin gallate (EGCG). Currently, the mechanism underlying the sensation of astringent taste is not well understood. I observed by calcium imaging that the mouse intestinal endocrine cell line STC-1 responds to the astringent compound, EGCG. Among major catechins of green tea, EGCG was most effective at eliciting a response in this cell line. This cellular response was not observed in HEK293T or 3T3 cells. Further analyses demonstrated that the 67-kDa laminin receptor, a known EGCG receptor, is not erectly involved. The $[Ca^{2+}]_i$ response EGCG in STC-1 cells was decreased by inhibitors of the transient receptor potential A1 channel (TRPA1). HEK293T cells transfected with the mouse TRPA1 cDNA showed a Ca^{2+} response upon application of EGCG, and their response properties were similar to those observed in STC-1 cells. These results indicate that an astringent compound, EGCG, activates the mouse TRPA1 in intestinal STC-1 cells. TRPA1 might play an important role in the astringency taste on the tongue.

Introduction

Tastants are detected mainly by taste receptor cells (TRCs) in taste buds on the tongue. Among the 5 basic taste stimuli, sweet, umami, and bitter taste are recognized by G protein-coupled receptors (GPCRs) (Chandrashekar et al., 2000; Nelson et al., 2001; Nelson et al., 2002; Chandrashekar et al., 2006; Ishimaru, 2009). As a candidate sour taste receptor, the heteromer of TRP (transient receptor potential) channels (PKD1L3 and PKD2L1) has been identified (Ishimaru et al., 2006; Huang et al., 2006). In the case of salty taste, epithelial Na^+ channels have been identified as amiloride-sensitive salty receptors, and are considered to play a role at least partly (Chandrashekar et al., 2006; Ishimaru, 2009). In addition to the 5 basic taste stimuli, the pungent stimulation of hot peppers is also recognized in the mouth. This pungent taste is mainly mediated by TRPV1 receptors, which can be activated by capsaicin from pepper and are expressed in TRCs and sensory neurons in the oral cavity (Ishida et al., 2002). Further, in beverages such as tea, cider, and red wine, as well as in several types of fruits, nuts, and chocolate, a characteristic astringent taste is elicited primarily by compounds known as polyphenols. Of these polyphenols, catechin, epicatechin (EC), epigallocatechin (EGC), epicatechin gallate (ECG), and epigallocatechin gallate (EGCG), and their polymers are most abundant in wine and tea. A typical green tea polyphenol is EGCG (Drewnowski and Gomez-Carneros, 2000; Lesschaeve and Nobel, 2005). Although recent reports demonstrated that a bitter taste receptor, hTAS2R39, is an oral sensor of EGCG (Slack et al., 2010, Narukawa et al., 2011), the mechanism underlying the sensation of astringent taste is not well understood.

Green tea has been shown to have anti-cancer activity in many organs (Yang et al., 2006; Bettuzzi et al., 2006). Among constituents of green tea, EGCG is the major polyphenol and exhibits the greatest cancer-preventive effects (Chung et al., 1999; Saeki et al., 2000). Recently, Tachibana et al. have found that the 67-kDa laminin receptor

(67LR) functions as a cell surface EGCG receptor inducing anti-cancer action (Tachibana et al., 2004). 67LR is a no integrin-type laminin receptor and expressed on a variety of tumor cells. Further, EGCG has been shown to induce the disruption of actin fibers and the dephosphorylation of the myosin II regulatory light chain through the 67LR to inhibit the growth of cancer cells (Umeda et al., 2005). Since activation of 67LR with EGCG does not influence the intracellular Ca^{2+} ($[Ca^{2+}]_i$) level (Fujimura et al., 2006), it seems that the EGCG signaling using 67LR may not induce the astringent sensation in sensory terminals in the oral cavity. Other receptor molecule for EGCG must be present as an astringent sensor on the tongue.

In addition to the gustatory system, chemosensory information perceived during the gastric and intestinal phases of digestion is important for the control of gastrointestinal function, such as the secretory activity of gastrointestinal glands, the restorative activity, motility and blood supply of the intestinal tract, and satiation (Dockray, 2003). The enteroendocrine cells are specialized transducers of luminal factors. STC-1 cells were established in 1990 as a line of enteroendocrine cells (Rindi et al., 1990). A decade later, Wu et al. reported that STC-1 cells express T2R bitter taste receptors and respond to bitter taste substances (Wu et al., 2002). We also characterized the bitter taste responses of STC-1 cells (Masuho et al., 2005). Then, we recently investigated the cellular responses of intestinal STC-1 cells to compounds of five basic tastants using a calcium-imaging technique. Although this cell line was known to respond to bitter compounds, we found that compounds of four other basic tastants also stimulated STC-1 cells. When solutions containing glutamate, sucrose, HCl, or NaCl were applied, the $[Ca^{2+}]_i$ concentration in STC-1 cells significantly increased. Therefore, we demonstrated that the gastrointestinal system can sense all five of the basic taste stimuli, and that it might contain a taste receptor signaling system similar to the oral taste system (Saitoh et al., 2007). The expression of T1R taste

receptors in the gut cells has also been reported by Dyer et al. (2005) and Margolskee et al. (2007).

Here, we investigated whether the intestinal STC-1 can respond to the astringent compound of green tea, EGCG, by the calcium-imaging technique. Interestingly, the results clearly indicated that STC-1 cells have a novel sensor for EGCG, which has not been described. When EGCG was applied to STC-1, a significant increase in the $[Ca^{2+}]_i$ concentration occurred. This cellular response was not observed in HEK293T or 3T3 cells, both of which express 67LR. Using some channel blockers, we focused on members of the transient receptor potential (TRP) channels and found that mouse TRPA1 (mTRPA1) is utilized in the EGCG-induced $[Ca^{2+}]_i$ response in STC-1 cells. Then, we characterized the responding properties of heterologously expressed mTRPA1 to EGCG in HEK293T cells.

Materials and Methods

Materials

(-)-epigallocatechin-3-gallate (EGCG), (-)-epicatechin (EC), (-)-epicatechin gallate (ECG), (-)-epigallocatechin (EGC), sodium L-glutamate (Glu-Na), menthol, capsaicin and sodium saccharin were from Wako (Osaka, Japan).   Caffeine, ruthenium red (R.R.) and $GdCl_3$ were from Sigma-Aldrich (St. Louis, MO).   AP-18 and HC-030031 were from Enzo Life Sciences (Plymouth Meeting, PA).   Denatonium benzoate was from Fluka (via Sigma-Aldrich).   Fluo8-AM was from AAT Bioquest (Sunnyvale, CA) and Rhodamine-phalloidin was from Molecular Probes (via Invitrogen, Carlsbad, CA).   Growth Factor Reduced MATRIGEL® Matrix (Matrigel) was from Becton Dickinson (Franklin Lakes, NJ).   The STC-1 cell line was a gift from Dr. D. Hanahan (University of California, San Francisco, CA).   The expression vector for mouse TRPA1 was previously described (Nagatomo and Kubo, 2008), and the vectors for rat TRPM8 and rat TRPV1 were provided by David Julius (University of California, San Francisco).

Culture and calcium imaging analysis of STC-1 cells

A culture medium consisting of DMEM supplemented with 10% FBS and antibiotics (100 μg/ml kanamycin) was used for STC-1 and HEK293T cells.   For 3T3 cells, newborn calf serum was added to the culture medium instead of FBS.   For calcium-imaging analysis, cells grown on a Matrigel-coated μ-Slide 8 well (80826, ibidi, MPI für Infektionsbiologie, Berlin, Germany) were washed with HBSS (Hanks' balanced salts solution; Sigma-Aldrich) and then incubated in HBSS containing 5 μM Fluo8-AM for 30 min at room temperature. Cells were then washed with HBSS and left at room temperature for an additional 30 min to allow cleavage of the AM ester.   Each recording chamber was filled with 150 μl of HBSS. To achieve abrupt changes in ligand concentration, 150 μl of 200% concentrated ligand

solution was applied by pipette. $[Ca^{2+}]_i$ was monitored at 470 nm Fluo8 emission excited by illumination at 525 nm using Axiovert 200 (Carl Zeiss, Gottingen, Germany).   Fluo8 fluorescence was recorded usually every 3 s and changes of fluorescence intensity were analyzed by Image-Pro Plus imaging software (Media Cybernetics, Silver Springs, MD). The mean fluorescence from at least five cells was obtained and the signals were expressed as the relative change in fluorescence: $\Delta F/F = (F-F_0)/F_0$.   All calcium imaging experiments were repeated two or three times.   For heterologous expression, HEK293T cells were transfected with the expression vector using Effectene transfection reagent (Qiagen, Chatsworth, CA). After 24-48 hours, cells were examined by the calcium-imaging technique. For experiments for the expression of TRPA1, cells were incubated in 3 μM R.R. for 24-48 hours, then washed with HBSS and used for the calcium imaging.

RT-PCR assay

Total RNA was isolated from cultured cells using TRIzol reagent (Invitrogen) and subjected to reverse transcription with random primers.   The reverse-transcribed cDNA was used as a template for PCR.   Total RNA treated under the same conditions without reverse-transcriptase was used as a negative control.   The primers used were as follows: for mouse 67-Da laminin receptor,

5'-TAAACCTGAAGAGGACCTGG-3' and 5'-GGTCCATTCACCCTGGAATT-3';

for mouse TRPA1,

5'-CATCTTCGTGTTGCCCTTGT-3' and 5'-AAAAACCGTAGCATCCTGCC -3';

for human TRPA1,

5'- CATTTTTGTGCTGCCCTTGT-3' and 5'-GGAATAACATCCCACCAGA-3';

for mouse TRPV1,

 5'-TCAGCCATCGCAAGGAGTAT-3' and 5'-CAGTTCACCTCATCCACCCT-3';

for human TRPV1,

5'-TCAGCCACCTCAAGGAGTAT-3' and 5'-TTCACCTCGTCCACCCTGAA-3';

for mouse TRPM8,

5'-ACTGCAACCGCCTAAACATC-3' and 5'-TCGTGGGAAAGGAGTGTCAA -3';

and for human TRPM8,

5'- ACTGCAGCCGCCTCAATATC-3' and 5'-GGAAAAAGGAGGCGGTAAGA-3'

PCR products were analyzed on 1% agarose gels.

Fluorescent staining for actin fibers

Cells were fixed for 20 min in 4% paraformaldehyde in PBS at room temperature, washed with PBS, and permeabilized with 0.5% TritonX-100 in PBS. Then, cells were stained with Rhodamine-phalloidin for 1 hour at room temperature, washed with PBS, and mounted with Prolong Gold antifade reagent (Invitrogen). The specimens were observed and recorded with an Axiovert 200 microscope equipped with phase contrast and epifluorescence optics.

Results

Green tea polyphenol EGCG can stimulate intestinal STC-1 cells

I previously demonstrated that intestinal STC-1 cells can sense all of the five basic taste stimuli and that a taste receptor signaling mechanism similar to the oral taste system might be present (Saitoh et al., 2007).   Here, I investigated whether this intestinal STC-1 might be able to respond to the major astringent compound of green tea, (-)-epigallocatechin- 3-gallate (EGCG), by means of the calcium-imaging technique. Approximately 1.5 mM EGCG is known to be present in standard green tea (Wang et al., 1992; Wolfram, 2007).   Addition of 200 μM EGCG to cultures of STC-1 cells, loaded with the fluorescence Ca^{2+} indicator Flou8- AM, induced a significant but relatively slow elevation in $[Ca^{2+}]_i$.   The responses to EGCG of STC-1 cells were dose-dependent, and quite low activation was detected at 20 μM EGCG (Fig. 1A).   On the other hand, when 3T3 or HEK293T cells were stimulated by 200 μM EGCG, no significant calcium elevation was observed (Fig. 1C and D).   EGCG is the most abundant green tea polyphenol.   In addition to EGCG, epicatechin (EC), epicatechin gallate (ECG) and epigallocatechin (EGC) are also present and generally known as tea catechins.   The effects of these catechins on the $[Ca^{2+}]_i$ of STC-1 cells were further examined.   As shown in Fig. 1E, each of these catechins induced a different level of stimulation of STC-1 cells at 200 μM.   The order of potency of these catechins was EGCG>EGC>ECG>EC.   The results indicated that EGCG was the most effective at inducing a Ca^{2+} response in STC-1 cells.

67LR-mediated signaling is not involved in the EGCG response of STC-1

Among the green tea constituents; EGCG is the most active constituent in inhibiting experimental carcinogenesis and related reactions.   67LR has been shown to function as a cell surface EGCG receptor to mediate the anticancer action of EGCG (Tachibana et al.,

2004).   Activation of 67LR by EGCG induces the disruption of stress fibers with actin cytoskeleton rearrangement and growth inhibition in cancer cells (Umeda et al., 2005; Umeda et al., 2008).   I next investigated whether 67LR-mediated signaling is involved in the EGCG response observed in intestinal STC-1 cells.   First, I examined the expression of 67LR mRNA by RT-PCR analysis.   Total RNA was isolated from STC-1, HEK293T, and 3T3 cells, and the reverse-transcribed cDNA with random primers was used as a template for PCR.   As shown in Fig. 2A, 67LR mRNA appeared to be expressed in all cell lines examined.   I further studied the effects of EGCG on the actin cytoskeleton.   To visualize the distribution of F-actin structures, fluorescently labeled phalloidin was utilized.   As a control, I first examined HEK293T cells.   I observed that HEK293T cells showed no significant elevation of $[Ca^{2+}]_i$ after the treatment with EGCG, and that 67LR mRNA was expressed in this cell line.   When HEK293T cells were treated with 200 μM EGCG, disappearance of actin fibers in the central body of cells occurred 2 min after the addition of EGCG and only the cell-cell junctions were weakly visible at 4 min after the EGCG addition.   On the other hand, when STC-1 cells were treated with 200 μM EGCG, interestingly, actin fibers were newly formed 2 min upon treatment with EGCG and the fiber formation continued for at least 4 min.   As a result, the intensity of phalloidin staining in STC-1 cells appeared to increase after the EGCG treatment (Fig. 2B).   This effect on actin fibers was observed from 50 μM EGCG.   Thus, I found that the effects of EGCG on the actin cytoskeletal structures were completely opposite in HEK293T and STC-1 cells, suggesting that the 67LR-mediated signaling observed in many cancer cells might not be involved in the mechanism underlying the EGCG-induced response of $[Ca^{2+}]_i$ elevation in STC-1 cells.

Possible involvement of the TRPA1 channel in the EGCG response of STC-1

To determine the contribution of Ca^{2+} influx through the plasma membranes from the extracellular medium on the increase in Ca^{2+} induced by EGCG in STC-1 cells, I performed calcium imaging using Ca^{2+}-free HBSS as the bath solution. As shown in Fig. 3A, the response was completely abolished in the absence of Ca^{2+}_{o}. This result indicated that Ca^{2+}_{o} is responsible for a major component of the increase in $[Ca^{2+}]_i$ induced by EGCG. Further, the effects of blockers for transient receptor potential (TRP) channels were studied. Gd^{3+} or R.R. significantly inhibited the Ca^{2+} response in STC-1 cells (Fig. 3B). The results suggested that TRP channels might be involved in the unique response of STC-1 cells to EGCG. Among TRP channels, the TRPA1 channel is activated by various pungent compounds, such as isothiocyanates, allicin, cinnamaldehyde, menthol, and sanchol (Jordt et al., 2004; Bandell et al., 2004; Macpherson et al., 2005; Karashima et al., 2007; Bautista et al., 2008). It is possible that TRPA1 might be involved in the response to the astringent stimulus with EGCG. I next examined the effects of TRPA1-specific inhibitors, AP-18 and HC030031 (McNamara et al., 2007; Petrus et al., 2007; Kerstein et al., 2009), on the Ca^{2+} response induced by EGCG in STC-1 cells. In the presence of AP-18 or HC030031, the EGCG-induced response was completely attenuated (Fig. 3C). I further investigated the expression levels of mRNAs of TRPA1, TRPV1, and TRPM8 in STC-1 cells by RT-PCR analysis. A significant expression of TRPA1 mRNA was detected, and low levels of TRPV1 mRNA were also detected (Fig. 3D). Treatment with capsaicin could not activate STC-1 cells, when examined using the calcium-imaging technique (Fig. 3E). The results strongly suggested that EGCG might activate TRPA1 channels to induce an increase in $[Ca^{2+}]_i$ in STC-1 cells. Although a low level of TRPV1 was also detected in HEK293T cells (Fig. 3D right panel), capsaicin could not activate HEK293T cells (Fig. 4C).

HEK293T cells respond to EGCG when expressing mTRPA1 channels

I next measured $[Ca^{2+}]_i$ in HEK293T cells expressing mouse TRPA1 (mTRPA1) channels. The expression vector for mTRPA1 cDNA was transfected into HEK293T cells, and the effect of EGCG on $[Ca^{2+}]_i$ was examined. I observed that 200 μM EGCG induced an increase in $[Ca^{2+}]_i$ in cells transfected with mTRPA1 cDNA, but not in cells transfected with the empty vector (Fig. 4A). TRPV1 and TRPM8 are known to have some features in common with TRPA1 (Jordt et al., 2004; Macpherson et al., 2005). HEK293T cells were transfected with the expression vectors of rat TRPV1 (rTAPV1) and rat TRPM8 (rTRPM8), and their responses to EGCG were also studied. A significant response was not observed in HEK293T cells expressing rTRPM8, but quite interestingly, the $[Ca^{2+}]_i$ -response was also induced in HEK293T cells expressing rTRPV1 (Fig. 4B and C). Since TRPV1 does not function in STC-1 cells, it is considered that the mTRPA1 channel mainly contributes to the response to EGCG observed in STC-1 cells.

Characterization of the response to tea catechins of HEK293T cells expressing mTRPA1 channels

I next examined the responses of HEK293T cells expressing mTRPA1 to various doses of EGCG. The results are shown in Fig. 5A and B. Significant activation was observed with 100 μM and 200 μM EGCG. Next, I examined the effects of 200 μM of other tea catechins on $[Ca^{2+}]_i$ in HEK293T cells expressing mTRPA1 (Fig. 5C). The order of potency of these catechins was EGCG>EGC>ECG>>EC. The results indicated that EGCG was the most effective activator among the green tea catechins, and demonstrated that the responses of HEK293T cells expressing mTRPA1 channels to catechins were very close to those observed with STC-1 cells. To assess the role of mTRPA1 in the response to EGCG, I investigated the effects of TRP channel blockers. First, to determine the

contribution of Ca^{2+} influx to the response of $[Ca^{2+}]_i$ induced by EGCG observed in HEK293T cells expressing mTRPA1, I performed calcium imaging using Ca^{2+}-free HBSS as the bath solution.   The response was completely abolished in the absence of Ca^{2+}_o (Fig. 5D).   When a general blocker for TRP channels, Gd^{3+} or R.R., was present in the bath solution of HEK293T cells expressing mTRPA1, the increase in $[Ca^{2+}]_i$ induced by EGCG appeared to be inhibited (Fig. 5E).   It was previously reported that the response of HEK293T cells expressing mTRPA1 to caffeine was almost completely blocked by Gd^{3+} or R.R. (Nagatomo and Kubo, 2008), but the EGCG-induced response here was only partially inhibited by Gd^{3+} or R.R.   The variation might be due to e.g. the difference of the type and concentration of ligands, as seen in previous reports (Chen et al, 2007; McNamara et al, 2007; Maher et al, 2008).   I next investigated whether TRPA1-specific inhibitors, AP-18 and HC030031, could block the EGCG-induced response.   In the presence of AP-18 or HC-030031, EGCG could not induce a significant response in cells expressing mTRPA1 (Fig. 5F).

Activation of mTRPA1 with EGCG induces the formation of actin fibers

In HEK293T cells, actin fibers were disassembled after addition of EGCG, but in STC-1 cells, treatment with EGCG induced the new formation of actin fibers.   I next studied whether a TRPA1-specific inhibitor could block the EGCG-induced formation of actin fibers in STC-1 cells.   Again, to examine the distribution of F-actin structures, fluorescently labeled phalloidin was used.   As shown in Fig. 6, 200 μM EGCG enhanced the formation of actin fibers within 4 min.   However, in the presence of AP18, a TRPA1-specific inhibitor, formation of the actin cytoskeleton was not enhanced.   The results suggested that the EGCG treatment newly forms filamentous structures of actin through the activation of mTRPA1 in STC-1 cells.   From these several lines of evidence, it

was demonstrated that EGCG induces the activation of mTRPA1 in intestinal STC-1 cells, and it was suggested that the mTRPA1 channel may function as an EGCG sensor in STC-1 cells.

Discussion

EGCG response in STC-1 cells

In this study, I investigated whether the mouse intestinal cell line, STC-1, can respond to the astringent compound of green tea, EGCG. By using a calcium-imaging technique, I found that the $[Ca^{2+}]_i$ of STC-1 increases in response to EGCG. I previously showed that all five of the basic taste stimuli induced an elevation of $[Ca^{2+}]_i$ in intestinal STC-1 cells (Saitoh et al., 2007). When the time courses of the elevations of $[Ca^{2+}]_i$ were compared, the response to EGCG, interestingly, appeared to be slower than that to any of the five basic taste stimuli. All of the responses to the five basic taste stimuli reached the maximum level within 30-60 s in STC-1 cells. On the other hand, incubation for more than 120 s was required to reach the maximum level for the EGCG-induced increase in $[Ca^{2+}]_i$. It was considered that the EGCG treatment indeed triggers a distinct mechanism in STC-1 cells. This cellular response was not observed in HEK293T or 3T3 cells, both of which express 67LR functioning as a cell surface EGCG receptor inducing anti-cancer action (Tachibana et al., 2004).

I further studied the effects of EGCG on the actin cytoskeleton of STC-1 cells and observed that actin stress fibers were newly formed upon treatment with EGCG. In HEK293T cells, however, actin fibers disappeared after the addition of EGCG, as previously reported (Umeda et al., 2005). It has also been reported that EGCG reduces phosphorylation of the myosin regulatory light chain (MRLC) of myosin II through 67LR and eukaryotic translation elongation factor 1A (eEF1A) to induce rearrangement of the actin cytoskeleton in cancer cells (Umeda et al., 2008). It is possible that the increase in $[Ca^{2+}]_i$ might elevate the phosphorylation of MRLC by Ca^{2+}/calmodulin-dependent myosin light-chain kinase in STC-1 cells (Citi and Kendric-Jones, 1987). The phosphorylation of MRLC might lead to a conformational change in myosin II, enabling it to assemble into filaments, and might

promote the formation of stress fibers (Chrzanowska-Wodnicka and Burridge, 1996). Such actin fiber formations have been reported to occur within 5 min (Ridley and Hall, 1992; Chrzanowska-Wodnicka and Burridge, 1996). It is known that compounds present in the gastrointestinal (GI) tract activate the secretion of GI hormones such as cholecystokinin from STC-1 cells (Chen et al., 2006). Therefore, the formation of stress fibers by EGCG may also contribute to the secretion of GI hormones. To examine this point, further detailed experiments are required.

The present results strongly suggested that a novel sensor molecule is present on the surface of STC-1 cells. I showed that TRPA1-specific inhibitors, AP-18 and HC-030031, attenuated the Ca^{2+} response and the increase in actin fibers in EGCG-treated STC-1 cells. Since the inhibition with either blocker was almost complete, it was considered that mouse TRPA1 might be a main contributor, and that other channels or receptors may not contribute to the EGCG-activation of STC-1 cells. It was reported recently that the human bitter taste receptor hTAS2R39 responds to tea catechins (Narukawa et al., 2011). In that report, the authors found that the strongest response was observed with ECG, followed in order by EGCG, EC, and EGC. On other hand, in the present study I demonstrated that the order of potency of tea catechins to activate STC-1 cells or mTRPA1 channels was EGCG > EGC > ECG > EC. Therefore, it is considered that the mouse homologue of hTAS2R39 may not mediate the response of STC-1 to tea catechins.

I observed a high-level expression of TRPA1 mRNA in STC-1 cells. In addition, I detected a low-level expression of TRPV1 mRNA. However, an agonist of TRPV1, capsaicin, could not induce any Ca^{2+} response in STC-1 cells. The expression level of TRPV1 may be quite low or the channel activity of TRPV1 might be blocked by an unknown mechanism in STC-1 cells. At least, it seems that TRPV1 does not contribute to the EGCG-induced response observed in STC-1 cells.

Expression of mTRPA1 channels converts cells to respond to the astringent stimulus with EGCG

MouseTRPA1 (mTRPA1) channel was expressed in the HEK293T cells, which normally cannot respond to EGCG, as a candidate sensor for EGCG. The transfected cells could be activated by EGCG with the characteristic slow time course observed in STC-1 cells and in a dose-dependent manner similarly to STC-1 cells. I also found that the order of potency of the four green tea catechins (EGCG, EGC, ECG, EC) to activate mTRPA1 was very close to the order observed using STC-1 cells. Finally, the activation with EGCG of HEK293T cells expressing mTRPA1 was abolished in the presence of AP-18 or HC-030031. These results clearly demonstrated that the mTRPA1 channel is required for and functions in the EGCG-induced response in intestinal STC-1 cells. Furthermore, HEK cells expressing rTRPV1 also could be activated with EGCG. Compared with the rapid response to capsaicin, the activation time course for the EGCG response of rTRPV1 appeared to be as slow as that for mTRPA1. The mechanism for the EGCG-induced slow response is currently unknown. Although further investigation is required, it is possible that some signaling process might be activated to induce gradual elevation of $[Ca^{2+}]_i$ after initial activation of TRP channels with EGCG.

The EGCG treatment activates 67 LR but cannot induce the elevation of $[Ca^{2+}]_i$ in cells other than STC-1 cells. However, it is possible that the presence of 67LR might be required for the EGCG-induced elevation of $[Ca^{2+}]_i$ in the cells expressing mTRPA1 or rTRPV1. I could not exclude this possibility. To examine this point, cell lines specifically lacking the expression of 67LR or 67LR-KO cells are required. Further, I examined the response to EGCG of *Xenopus* oocytes expressing mTRPA1 under two electrode voltage clamps. I tried to record the current through mTRPA1 channels itself in the absence of extracellular Ca^{2+}, and also the Ca^{2+}-Cl^- current activated by Ca^{2+} influx through TRPA1 channels in the presence of

extracellular Ca^{2+}.　I could not detect any clear changes of the membrane current in either case (data not shown), although positive control responses to AITC were clearly observed. The results suggest that additional protein factors endogenously present in HEK cells might be required for mTRPA1 to constitute a functional sensing system of EGCG, or that post-translational modifications that occur only in mammalian cells might be essential for mTRPA1 to recognize EGCG.

A characteristic oral astringent taste is elicited primarily by polyphenols.　Of these polyphenols, EGC, ECG, and EGCG are present in wine and tea.　A typical green tea polyphenol is EGCG　(Drewnowski and Gomez-Carneros, 2000; Lesschaeve and Nobel, 2005).　The mechanism underlying the sensation of the astringent taste, however, is not well-known.　Here, I first demonstrated that the intestinal STC-1 cells can be activated with EGCG, and that EGCG can stimulate HEK293T cells expressing mTRPA1 channels.　It is known that typical green tea contains -1.5 mM EGCG (Wang et al., 1992; Wolfram, 2007). Therefore, our results clearly indicate that the EGCG present in green tea can activate mTRPA1 on the cell surface.　TRPA1 is a member of the TRP family of ion channels and expressed in a subset of nociceptive neurons.　Recently, it has been reported that this TRP channel protein is expressed in the nerve fibers in the mouse tongue (Nagatomo and Kubo, 2008).　Therefore, although further investigation is required, it is possible that mTRPA1 plays an important role in the sensation of astringency taste on the tongue.

Figure Legends

Fig. 1 Green tea polyphenol EGCG can stimulate intestinal STC-1 cells.

(A) STC-1 cells preloaded with 5 μM Fluo8-AM were challenged with 2 μM, 20 μM, 100 μM or 200 μM EGCG. The Fluo8 fluorescence was recorded every 3 s and the relative fluorescence change (ΔF/F) was determined as described in the Materials and Methods. At 9 s, the ligand was applied to the bath.

(B) As shown in A, STC-1 cells were stimulated with various doses of EGCG and the dose-response relationship was observed. The means of ΔF/F at 237 s after ligand stimulation are plotted.

(C) STC-1 or 3T3 cells preloaded with 5 μM Fluo8-AM were activated with 200 μM EGCG. The Fluo8 fluorescence was recorded every 3 s and ΔF/F was analyzed. At 9 s, the ligand was applied to the bath.

(D) STC-1 or HEK293T cells preloaded with 5 μM Fluo8-AM were stimulated with 200 μM EGCG. The Fluo8 fluorescence was recorded every 3 s and ΔF/F was analyzed. At 9 s, the ligand was applied to the bath.

(E) STC-1 cells preloaded with 5 μM Fluo8-AM were stimulated with 200 μM of EGCG, EC, ECG or EGC. The Fluo8 fluorescence was recorded every 6 s and ΔF/F was analyzed. The average ΔF/F at 231 s after ligand stimulation is shown. Differences judged to be significant by the Tukey-Kramer method are marked with one to three asterisks as follows: *$P<0.05$, **$P<0.01$, ***$P<0.001$.

Fig. 2 67LR-mediated signaling is not involved in the EGCG response of STC-1.

(A) Expression of 67LR was examined in STC-1 cells. Total RNA was isolated from STC-1, HEK293T and 3T3 cells and RT-PCR analysis was performed using primers for 67LR as described in the Materials and Methods. When using the reaction mixture without reverse-transcriptase (RT (-)), no PCR product was observed.

(B) The effect of EGCG on the actin cytoskeleton organization in STC-1 cells was examined. STC-1 and HEK293T cells were cultured on Matrigel-coated coverslips and culture medium was replaced with HBSS before addition of EGCG.   At 0 min, 1 min, 2 min, 3 min and 4 min after stimulation with 200 μM EGCG, the cells were fixed and stained for actin fibers as described in the Materials and Methods.   All images were obtained with the same exposure time.

Fig. 3 Possible involvement of TRP channels in the EGCG response of STC-1.

(A) Effects of EGCG on $[Ca^{2+}]_i$ in the absence of Ca^{2+}_o were examined. $[Ca^{2+}]_i$ was monitored in STC-1 cells loaded with 5 μM Fluo8-AM in the presence or absence of Ca^{2+}_o. The Fluo8 fluorescence was recorded every 6 s and ΔF/F was analyzed.   At 6 s, 200 μM EGCG was applied to the bath.

(B) $[Ca^{2+}]_i$ was monitored in STC-1 cells loaded with 5 μM Fluo8-AM in the absence or the presence of 50 μM Gd^{3+} or 5 μM ruthenium red (R.R.).   The Fluo8 fluorescence was recorded every 3 s and ΔF/F was analyzed.   At 9 s, 50 μM EGCG was applied to the bath.

(C) $[Ca^{2+}]_i$ was monitored in STC-1 cells loaded with 5 μM Fluo8-AM in the absence or the presence of 100 μM AP-18 or 100 μM HC-030031.   The Fluo8 fluorescence was recorded every 3 s and ΔF/F was analyzed.   At 9 s, 100 μM EGCG was applied to the bath.

(D) Total RNA was isolated from STC-1, 3T3 and HEK293T cells. RT-PCR analysis was performed using primers for TRPA1, TRPM8, and TRPV1 as described in the Materials and Methods.   When using the reaction mixture without reverse-transcriptase (RT (-)), no PCR product was observed.   For mouse cells (STC-1 and 3T3), the estimated sizes of PCR products were 608 bp for TRPA1, 654 bp for TRPV1, and 617 bp for TRPM8.   For human cells (HEK293T), the estimated sizes of PCR products were 605 bp for TRPA1, 655 bp for TRPV1, and 618 bp for TRPM8.   The lanes labeled M contain DNA size markers (left panel: 10 kbp, 4 kbp, 2 kbp, 1 kbp, 0.5 kbp, and 0.1 kbp; right panel: 2 kbp, 1 kbp, 0.5 kbp, and 0.1 kbp).

(E) $[Ca^{2+}]_i$ was monitored in STC-1 cells loaded with 5 μM Fluo8-AM. The Fluo8 fluorescence was recorded every 3 s and ΔF/F was analyzed. At 9 s, 10 μM capsaicin was applied to the bath and 100 μM AITC was further applied at 249 s.

Fig. 4 EGCG can stimulate HEK293T cells expressing mTRPA1 channels.

(A) The effect of EGCG (200 μM) on $[Ca^{2+}]_i$ in HEK293T cells expressing mouse TRPA1 (mTRPA1) was examined. After transfection with the expression vector of mTRPA1, cells were loaded with 5 μM Fluo8-AM. The Fluo8 fluorescence was recorded and ΔF/F was analyzed. At 9 s, 200 μM EGCG was applied to the bath, and at 240 s, 100 μM AITC was further applied.

(B) The effect of EGCG (200 μM) on $[Ca^{2+}]_i$ in HEK293T cells expressing rat TRPM8 (rTRPM8) was examined. After transfection with the expression vector of rTRPM8, cells were loaded with 5 μM Fluo8-AM. The Fluo8 fluorescence was recorded and ΔF/F was analyzed. At 9 s, 200 μM EGCG was applied to the bath, and at 240 s, 400 μM menthol was further applied.

(C) Effect of EGCG (200 μM) on $[Ca^{2+}]_i$ in HEK293T cells expressing rat TRPV1 (rTRPV1) was examined. After transfection with the expression vector of rTRPV1, cells were loaded with 5 μM Fluo8-AM. The Fluo8 fluorescence was recorded and ΔF/F was analyzed. At 9 s, 200 μM EGCG was applied to the bath, and at 240 s, 10 μM capsaicin was further applied.

Fig. 5 Characterization of the response to tea catechins of HEK293T cells expressing mTRPA1.

(A) The effect of EGCG (2 μM, 20 μM, 100 μM, 200 μM) on $[Ca^{2+}]_i$ in HEK293T cells expressing mTRPA1 was examined. After transfection with the expression vector of mTRPA1, cells were loaded with 5 μM Fluo8-AM. The Fluo8 fluorescence was recorded and ΔF/F was analyzed. At 9 s, EGCG was applied to the bath, and at 240 s, 100 μM AITC

was further applied.

(B) As shown in panel A, HEK293T cells expressing mTRPA1 were stimulated with various doses of EGCG and the dose-response relationship was observed.   The means of $\Delta F/F$ at 237 s after ligand stimulation are plotted.

(C) HEK293T cells expressing mTRPA1 were preloaded with 5 μM Fluo8-AM and were stimulated with 200 μM of EGCG, EC, ECG or EGC.   The Fluo8 fluorescence was recorded every 6 s and $\Delta F/F$ was analyzed.   The average $\Delta F/F$ at 231 s after ligand stimulation is shown.   Differences were judged to be significant by the Tukey-Kramer method (* $P<0.05$, ***$P<0.001$).

(D) Effects of EGCG on $[Ca^{2+}]_i$ in the absence of Ca^{2+}_o were examined.   HEK293T cells expressing mTRPA1 were preloaded with 5 μM Fluo8-AM, and $[Ca^{2+}]_i$ was monitored in the presence or absence of Ca^{2+}_o after addition of EGCG.   The Fluo8 fluorescence was recorded every 3 s and $\Delta F/F$ was analyzed.   At 9 s, 200 μM EGCG was applied to the bath and at 240 s, 100 μM AITC in Ca^{2+}-containing HBSS was further applied.

(E) After transfection with the expression vector of mTRPA1, $[Ca^{2+}]_i$ was monitored in cells preloaded with 5 μM Fluo8-AM in the absence or the presence of 50 μM Gd^{3+} or 5 μM R.R. The Fluo8 fluorescence was recorded every 3 s and $\Delta F/F$ was analyzed.   At 9 s, 50 μM EGCG was applied to the bath.

(F) $[Ca^{2+}]_i$ was monitored in HEK293T cells expressing mTRPA1 in the absence or the presence of 100 μM AP-18 or 100 μM HC-030031.   The Fluo8 fluorescence was recorded every 3 s and $\Delta F/F$ was analyzed.   At 9 s, 100 μM EGCG was applied to the bath, and at 240 s, 100 μM AITC was further applied.

Fig. 6 Activation of mTRPA1 with EGCG induces the formation of actin fibers.

STC-1 cells were cultured on Matrigel-coated coverslips and culture medium was replaced with HBSS before addition of ligands.   At 4 min after stimulation with HBSS, 200 μM

EGCG, 100 µM AP-18, or 200 µM EGCG and 100 µM AP-18, the cells were fixed and stained for actin fibers as described in the Materials and Methods. All images were obtained with the same exposure time. Phase contrast (A, C, E, G) and fluorescent (B, D, F, H) images are shown.

Figure 1
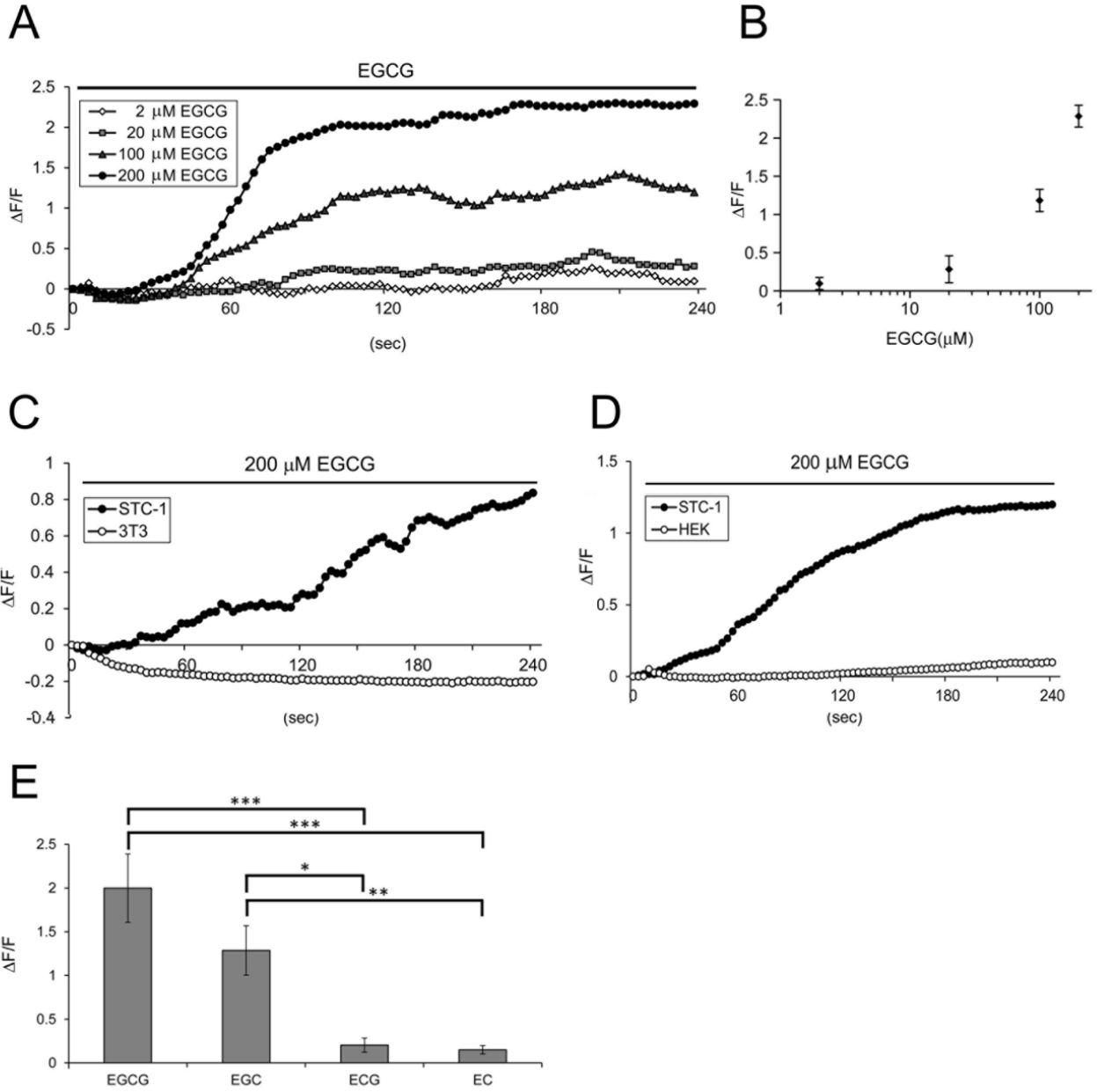
Figure 2
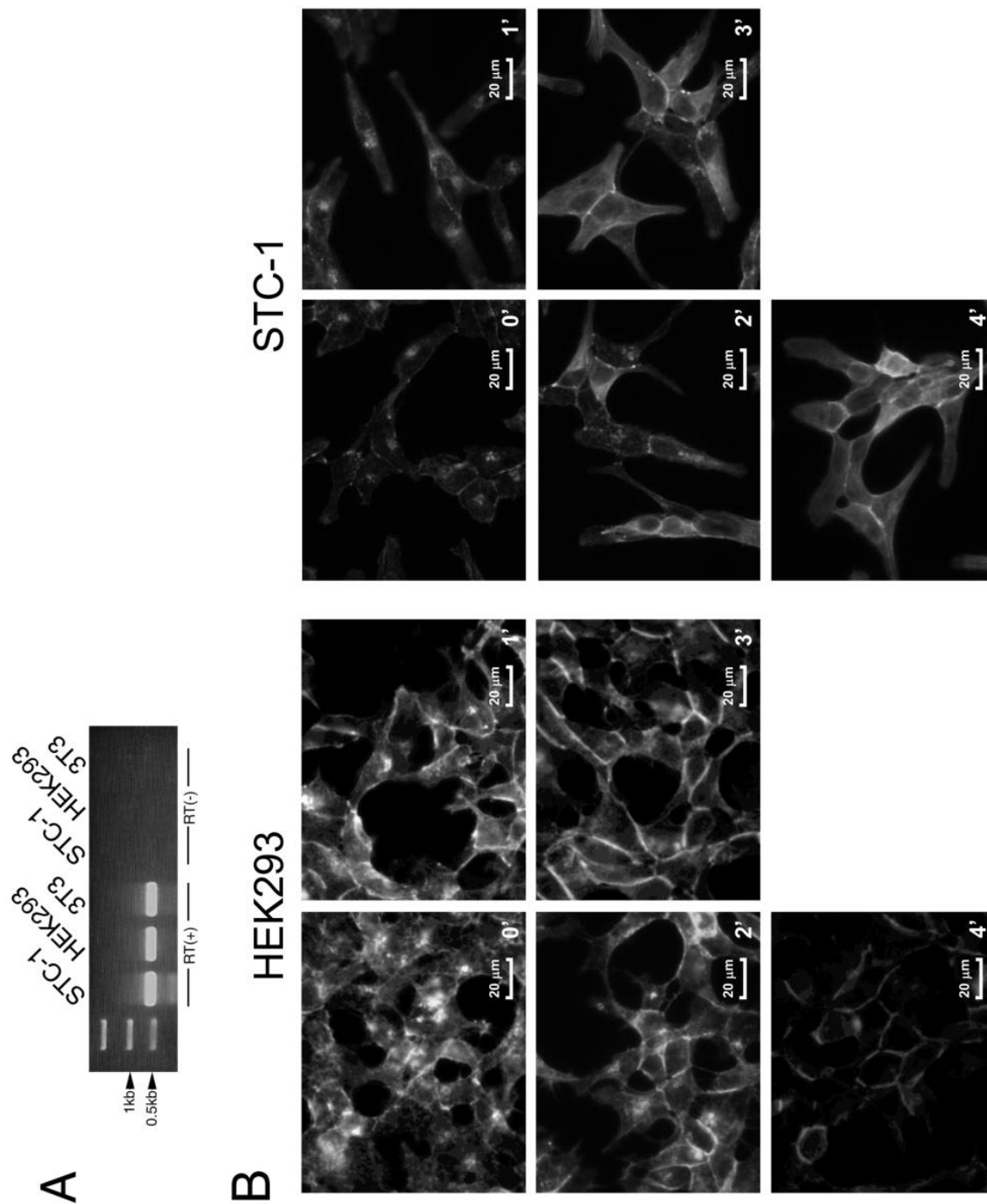
Figure 3
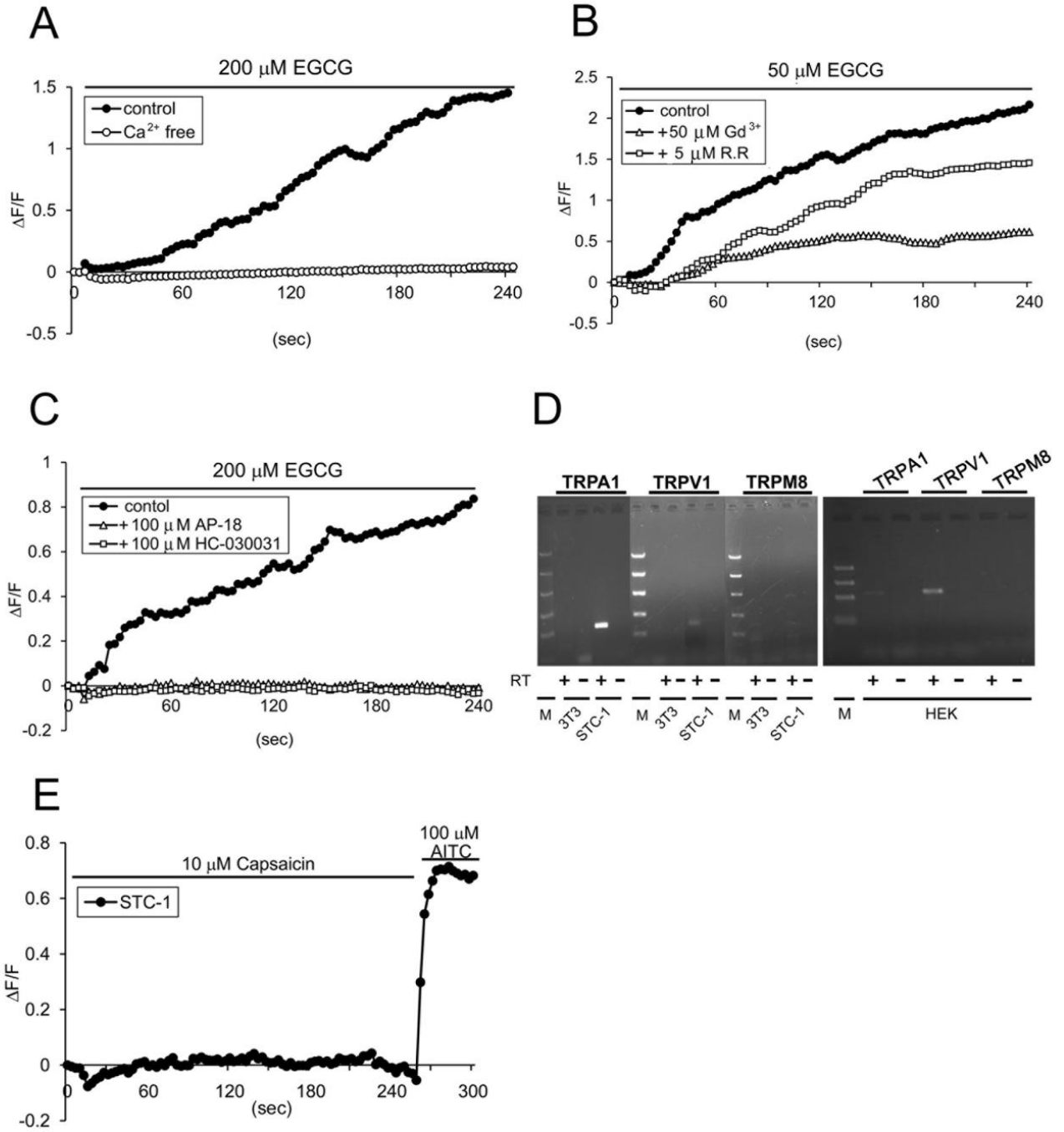
Figure 4
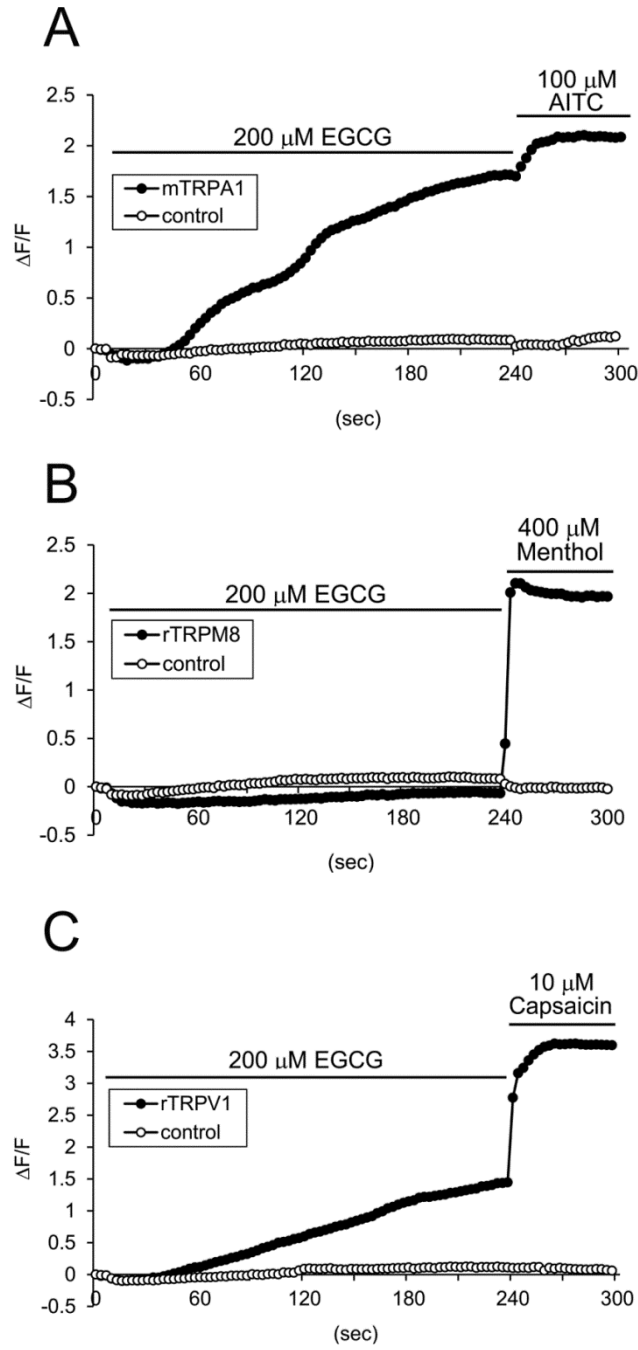
Figure 5
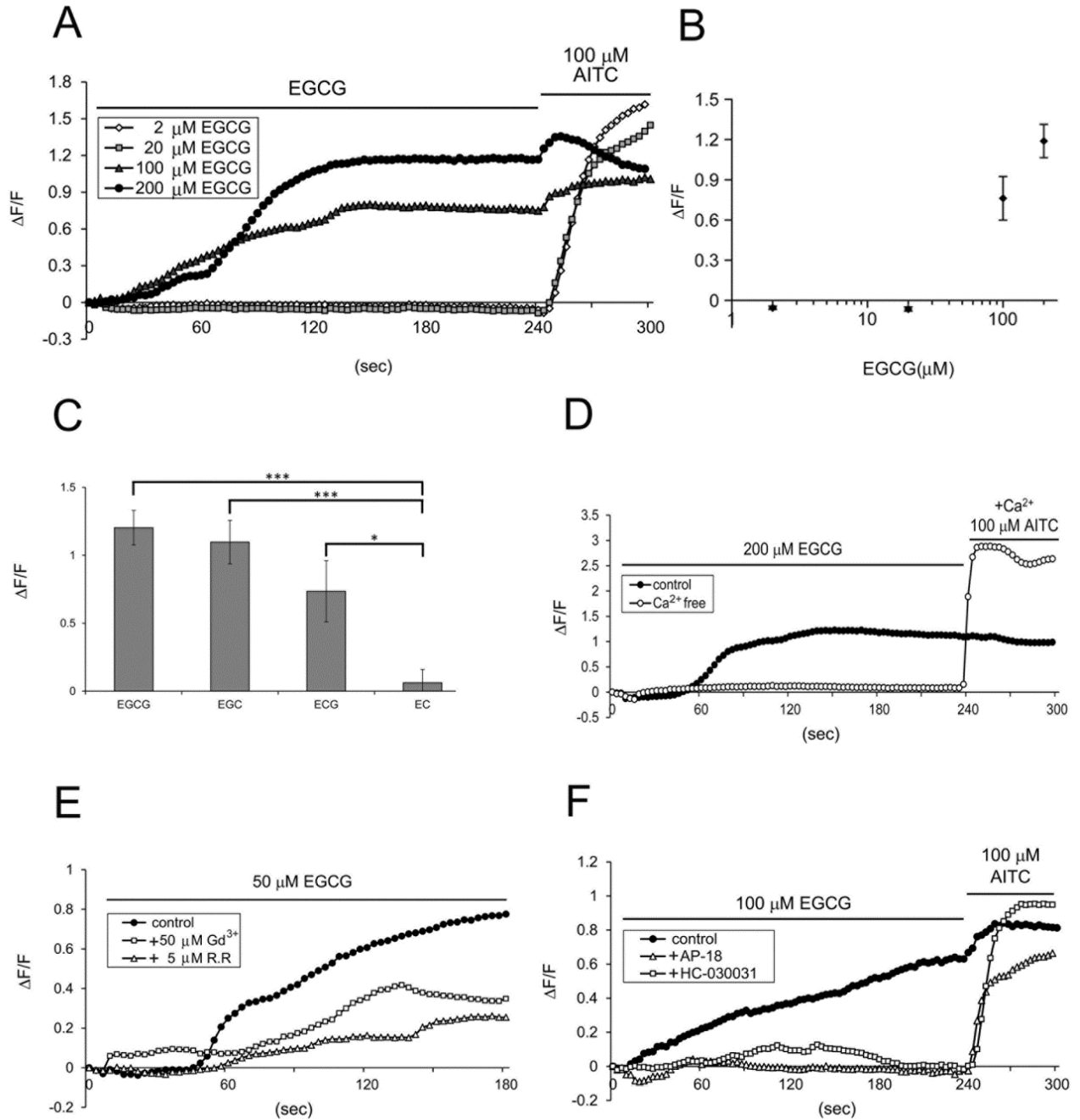
Figure 6
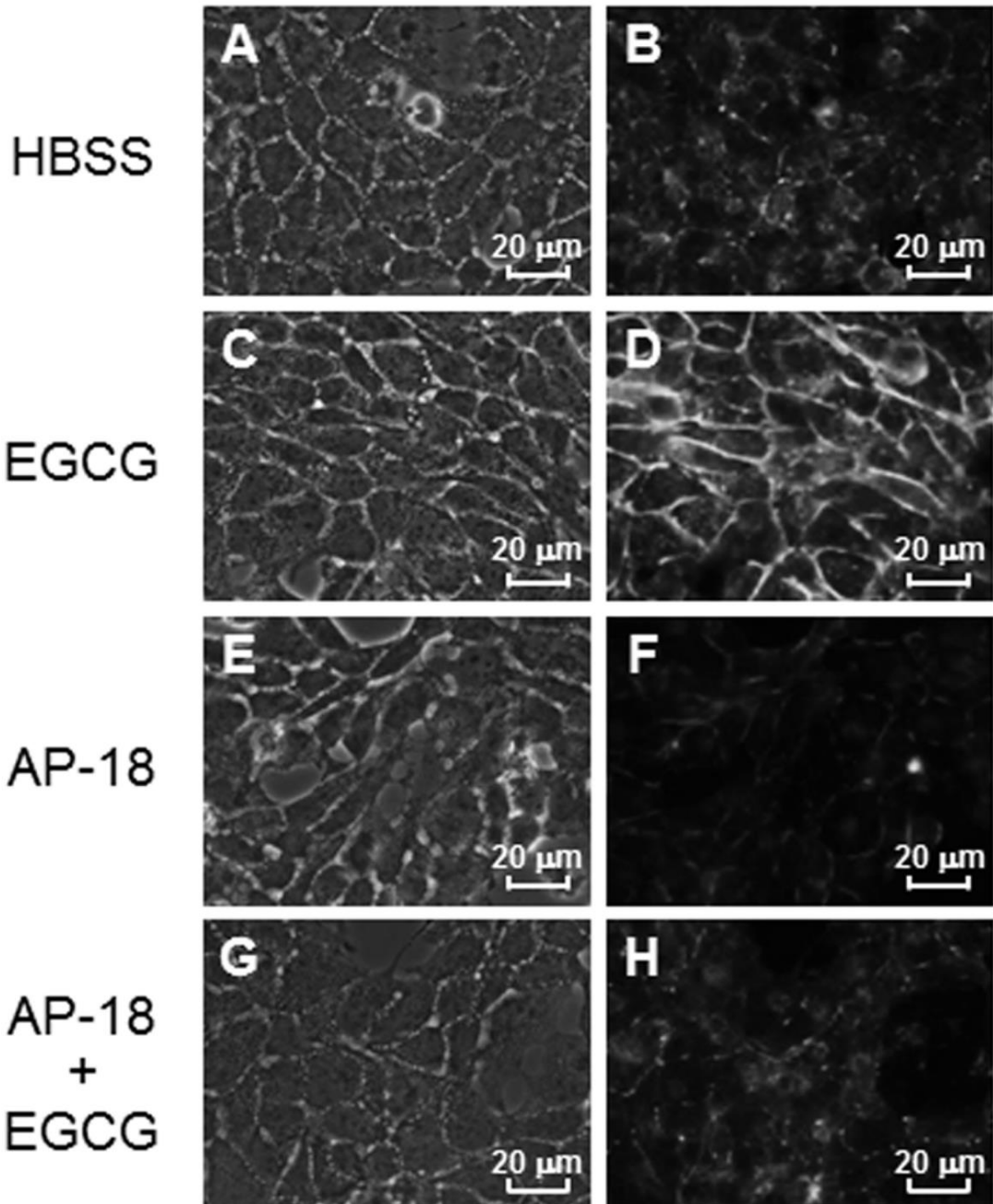
Chapter Ⅱ

Auto-oxidation products of epigallocatechin gallate activate

TRPA1 and TRPV1 in sensory neurons.

Abstract

The sensation of astringency is elicited by catechins and their polymers in wine and tea. It has been considered that catechins in green tea are unstable and auto-oxidized to induce more astringent taste. Here, we examined how mammalian transient receptor potential V1 (TRPV1) and TRPA1, which are nociceptive sensors expressed in nerve fibers in the tongue, are activated by green tea catechins during the auto-oxidation process. Neither TRPV1 nor TRPA1 could be activated by any of the freshly prepared catechin. When one of the major catechin, epigallocatechin gallate (EGCG) was pre-incubated for 3 hours in Hank's balanced salt solution, it, however, significantly activated both TRP channels. Even after incubation other catechins showed much less effects. Results suggest that only oxidative products of EGCG activate both TRPV1 and TRPA1. Dorsal root ganglion (DRG) sensory neurons were also activated by the incubated EGCG through TRPV1 and TRPA1 channels. Liquid chromatography/mass spectrometry revealed that theasinensins A and D (TS-A and TS-D) are formed during incubation of EGCG. We found that purified TS-A activates both TRPV1 and TRPA1, and that it stimulates DRG neurons through TRPV1 and TRPA1 channels. Results indicated that TRPV1 and TRPA1 channels play a critical role in the mechanism for astringent taste on the tongue.

Introduction

In addition to five basic taste stimuli (sweet, umami, salty, sour, bitter), the pungent stimulation of hot peppers is also recognized in the mouth. Such sensation is mainly mediated by TRPV1 (transient receptor potential V1) receptors (Caterina et al., 1997; Ishida et al., 2002). Further, in beverages such as tea, cider, and red wine, as well as in several types of fruits, nuts, and chocolate, a characteristic astringent sensation is elicited primarily by polyphenols. Of these polyphenols, catechin, epicatechin (EC), epigallocatechin (EGC), epicatechin gallate (ECG), and epigallocatechin gallate (EGCG), and their polymers are abundant in wine and tea. A most abundant green tea polyphenol is EGCG (Drewnowski and Gomez-Carneros, 2000; Lesschaeve and Nobel, 2005). Currently, the sensation mechanism for astringent taste induced by green tea polyphenols such as EGCG is not well understood.

Green tea has been shown to have anti-cancer activity in many organs (Yang et al., 2006; Bettuzzi et al., 2006), and EGCG is the major polyphenol with the cancer preventive effects (Chung et al., 1999; Saeki et al., 2000). Tachibana et al. have found that a 67-kDa laminin receptor (67LR) functions as a cell surface EGCG receptor inducing the anti-cancer action (Tachibana et al., 2004). EGCG has been shown to inhibit the growth of cancer cells through the 67LR (Umeda et al., 2005). It is considered that the EGCG signaling using 67LR may not induce the astringent sensation in sensory terminals in the oral cavity.

We previously found that the mouse intestinal endocrine cell line STC-1 can respond to EGCG among four major tea catechins by the calcium-imaging technique. We further indicated that EGCG stimulates intestinal STC-1 cells by activating TRPA1 channels. Since TRPA1 is more likely to be expressed in nerve fibers in the tongue, we demonstrated that TRPA1 might play an important role in the astringency taste on the tongue (Kurogi et al., 2012). In the same report, we showed that TRPV1 is also activated by EGCG. On

the other hand, it has been considered that green tea incubated for longer period tastes more astringent by auto-oxidation, and it was demonstrated that astringency increases with degree of polymerization of polyphenols (Peleg et al., 1999). EGCG is known to be auto-oxidized in neutral pH, and EGCG dimmers of theasinensins A / D (TS-A / TS-D) and P2 (another dimer with MW 884) have been reported to be formed (Hong et al., 2002). Furthermore, several biological activities have been reported for theasinensins (TSs) (Hou et al., 2005; Hou et al., 2010). How do these auto-oxidation products of EGCG affect TRPA1 and TRPV1 channels?

Here, we examined how TRPA1 and TRPV1 are activated by tea catechins in the course of auto-oxidation process. Interestingly, neither TRPA1 nor TRPV1 could be activated by one of the freshly prepared catechins without pre-incubation. EGCG pre-incubated for 3 hours in Hank's balanced salt solution (HBSS), however, significantly activated both TRP channels. The presence of ascorbic acid inhibited the pre-incubation effect on EGCG. In the previous experiments, the catechin solution was prepared before loading Ca^{2+} indicator dye to cells, and the solution was kept for about 30 min before assay. These results strongly suggested that only oxidative products of EGCG activate TRPA1 and TRPV1. Furthermore, we observed that DRG (dorsal root ganglion) neurons are activated by the pre-incubated EGCG through TRPV1 and TRPA1 channels. Then, we found that EGCG dimmers, TSs, are present in the incubated auto-oxidized EGCG. TS-A was synthesized and purified, and the activity to stimulate TRP channels was studied.

Materials and Methods

Experimental animals

All animal experiments described below conformed to the institutional guideline and were approved by the Animal Experiment Committee of Nagahama Institute of Bio-Science and Technology.

Materials

(-)-epigallocatechin-3-gallate (EGCG), (-)-epicatechin (EC), (-)-epicatechin gallate (ECG) and (-)-epigallocatechin (EGC), capsazepine (CPZ), and capsaicin were from Wako (Osaka, Japan).   Allyl isothiocyanate (AITC) was from Nacalai tesque (Kyoto, Japan). Ruthenium red (RR) was from Sigma-Aldrich (St. Louis, Missouri USA). 4-(4-Chlorophenyl)-3- ethylbut-3-en-2-oxime (AP-18) was from Enzo life sciences (Plymouse meeting, Pennsylvania, USA).   Fluo8-AM was from AAT Bioquest (Sunnyvale, California, USA).   Growth Factor Reduced MATRIGEL® Matrix (matrigel) was from Becton Dickinson (Franklin Lakes, New Jersey, USA).   The expression vector for mouse TRPA1 was previously described (Nagatomo and Kubo, 2008), and the vectors for rat TRPV1, rattlesnake TRPV1, rattlesnake TRPA1, and chick TRPV1 were provided by Dr. David Julius (UCSF, California, USA) and zebrafish TRPA1a and zebrafish TRPA1b were provided by Dr. Alexander F. Schier (ICCB, Massachusetts, USA).

Cell culture and calcium imaging analysis

The culture medium consisted of DMEM supplemented with 10% FBS and antibiotics (100 μg/ml kanamycin) was used for HEK293T cells.   For heterologous expression, HEK293T cells were transfected with the expression vector (TRPV1 or TRPA1) using Effectene transfection reagent (Qiagen, Chatsworth, California, USA).   After 24-48 hours, cells were examined by the calcium-imaging technique.   For the expression of TRPA1, cells

were incubated in 3 µM RR to increase viability for 24-48 hours, then washed with Hank's balanced salt solution (HBSS) and used for the calcium-imaging.

To establish primary cultures of DRG neurons, 6-10 week-old C57BL/6 mice were killed by cervical dislocation, after which the DRG were mechanically isolated. The isolated ganglia were dissociated and cultured as described (Dai et al., 2007). Using cells grown on matrigel-coated µ-Slide 8 well (80826, ibidi, MPI für Infektionsbiologie, Berlin, Germany), the calcium-imaging analysis with Fluo8-AM was performed as previously described (Kurogi et al., 2012). Fluo8 fluorescence was recorded every 3 s using Axiovert 200 (Carl Zeiss, Gottingen, Germany) and changes of fluorescence intensity were analyzed by Image-Pro Plus imaging software (Media Cybernetics, Silver Spring**,** Maryland, USA). The signals are expressed as relative fluorescence change: $\Delta F/F = (F-F_0)/F_0$. Various catechin samples were applied to cells at 6 s, and 10 µM capsaicin or 100 µM AITC was further applied at 240 s or 120 s to confirm the channel expression. When effects of channel blockers were examined, the solution of capsaicin or AITC was similarly applied without blockers at the end of the imaging to cancel the blocker effect. All calcium imaging experiments were repeated two or six times.

Immunohistochemistry.

The expression vector of rat TRPV1 or mouse TRPA1 was transfected into HEK293T cells. After transfection (24-48 hours), cells were fixed for 20 min in 4% paraformaldehyde in PBS at room temperature (r.t.), washed with PBS, and permeabilized with 0.1% TritonX-100 in PBS, and blocked for 1 hour at r.t. in PBS containing 1% skim milk. Then cells were incubated for 1 hour at r.t. with the appropriate primary antibody (rabbit anti-TRPV1 (Abcam, Cambridge, ENG) or rabbit anti-TRPA1 antibody(Nagatomo and Kubo, 2008)) in 1% skim milk − PBS, washed with PBS, and incubated with Alexa488

labelled anti-rabbit 2nd antibody in 10% Block Ace － PBS.   After washed with PBS, cells were mounted with Prolong Gold antifade reagent (Invitrogen).

Cultured mouse DRG cells were fixed, permeabilized, and blocked for 1 hour at r.t. in 1% skim milk － PBS.   First, cells were incubated for 1 hour at r.t. with mouse anti-Neurofirament (NF) antibody (IBL) in 1% Block Ace － PBS, washed with PBS, and incubated with Alexa568 labelled anti-mouse 2nd antibody in 1% Block Ace － PBS.   Then, cells were immunostained with rabbit anti-TRPV1 or rabbit anti-TRPA1 antibody. Immunoreation was further visualized with Alexa488 labelled anti-rabbit 2nd antibody. After washing with PBS, cells were mounted with Prolong Gold antifade reagent.

The specimens were observed and recorded with an Axiovert 200 microscope equipped with phase contrast and epifluorescence optics.

Molecular biology

Chick TRPA1 cDNA was cloned into the expression vector.   Total RNA was isolated from dorsal root ganglion (DRG) of 14 days chick embryo using TRIzol reagent (Invitrogen, Carlsbad, California, USA) and subjected to reverse transcription with random primers. The reverse-transcribed cDNA was used as a template of PCR.   Based on the predicted sequence of chick (*Gallus gallus*) TRPA1 mRNA (XM_418294), I used the following primers to amplify four overlapping DNA fragments of cDNA.

XbaI _chicTRPA1_2-f:

5'- TTTTTCTAGACTTAGTCCACCATGAAGCGCTCTCTGTGGC -3'

chicTRPA1_2r:

5'- TGCCAAATGAAGTGGACTGCACTTCCCATTATTGGT -3'

chicTRPA1_2f:

5'- ATAATGGGAAGTGCAGTCCACTTCATTTGGCAGTTC -3'

chicTRPA1_3r:

5'- CACAGAGAAAAGGGCCCCTCTTTTCAGAAGAAACT -3'

chicTRPA1_3f:

5'- TCTTCTGAAAAGAGGGGCCCTTTTTCTCTGTGACTA -3'

chicTRPA1_4r:

5'- CAGTCCAGTAGATTGGAGTAATCCAACAGATATTTC -3'

chicTRPA1_4f:

5'- TATCTGTTGGATTACTCCAATCTACTGGACTGGACA -3'

chicTRPA1_2 _ *XbaI* -r:

5'- GGGTCTAGATCACATAGAAGTCTACAATAAGC -3'

After subcloning and sequence confirmation of each cDNA fragment, a single

full-length cDNA fragment of chick TRPA1 (3393 bp) was amplified using these four

overlapping DNA fragments.　The resultant DNA was digested with *XbaI* and cloned into

XbaI-digested pcDNA3.1Hygro(-).　The orientation and the nucleotide sequence of cDNA

were further confirmed by sequencing analysis.

Liquid chromatography/electrospray ionization mass spectrometric (LC/MS) and tandem

MS (LC/MS/MS) analysis

Liquid chromatography/electrospray ionization mass spectrometric (LC/MS) and

tandem MS (LC/MS/MS) analyses were performed using a LCMS-IT-TOF (Shimadzu,

Kyoto, Japan).　Samples (10 μl, 4 mM) were applied to a Cosmosil $5C_{18}$-ARII column

(Nacalai Tesque Inc. Kyoto, Japan, 2.0 mm i.d. X 100 mm).　To elute the column, in the

first 15 min, the solvent was changed in a linear gradient from 90% A [0.1% formic acid]+

10% B [CH_3OH:CH_3CN=3:2] to 75% A + 25% B at a flow rate of 0.2 ml/min.　In the next

10min, the solvent was changed in a linear gradient to 40% A + 60% B.　Then, the solvent

was changed back to 90% A + 10% B and maintained at 90% A + 10% B for another 15min. The MS instrument was operated using an ESI source in negative ionization mode. Ionization parameters were as follows: probe voltage, 4.5kV; nebulizing gas flow, 1.5 L/min; CDL temperature, 200˚C; block heater temperature, 200°C.

Preparation of theasinensin A

TS-A was synthesized from EGCG and purified according to the method described by Shii et al (2011).   A solution of 5 mg EGCG and 0.01 mmol $CuCl_2$ in 30% MeOH (2 ml) was vigorously mixed at 25˚C for 16 hours.   To the mixture, 50 mg of AA was added and heated at 85˚C for 15 min.   After cooling, the mixture was 2.5 times diluted with H_2O and applied to a preparative HPLC using a Cosmosil $5C_{18}$-ARII column (Nacalai Tesque Inc. Kyoto, Japan, 20 mm i.d. X 250 mm).   To elute the column, in the first 50 min, the solvent was changed in a linear gradient from 90% A [H_2O] + 10% B [$CH_3OH:CH_3CN = 3:2$] to 75% A + 25% B at a flow rate of 3 ml/min.   In the next 20 min, the solvent was changed in a linear gradient to 40% A + 60% B and maintained at 40% A + 60% B for another 20 min. Then, the solvent was changed back to 90% A + 10% B and maintained at 90% A + 10% B for 60 min.   LC chromatograms were obtained at UV 254 nm.   The fraction TS-A was collected and concentrated by evaporation, and kept at -80˚C.   Purified TS-A was re-dissolved in HBSS containing 4 mM AA to block further auto-oxidization.

Results

Auto-oxidation products of EGCG activate TRPV1 and TRPA1 channels

To examine how EGCG activates TRPV1 and TRPA1 channels in the course of auto-oxidation process, I compared effects of freshly prepared and incubated EGCG on both channels.   HEK293T cells were transfected with the TRPV1 or TRPA1 expression vector and calcium-imaging analysis was performed.   EGCG was dissolved in Hank's balanced salt solution (HBSS) at 200 μM and incubated at 25°C for 2-6 hours, or freshly prepared just before use.   I did not observe a significant increase in $[Ca^{2+}]_i$ in HEK293 cells expressing TRPV1 or TRPA1 with the freshly prepared EGCG. However, following incubation, EGCG could induce an increase in $[Ca^{2+}]_i$ in cells expressing either TRP channels.   When EGCG was incubated in the presence of an antioxidant, 1 mM AA, the increase in $[Ca^{2+}]_i$ was not induced by the EGCG in HEK293T cells expressing TRPV1 or TRPA1 channels (Fig. 1). Results demonstrated that auto-oxidation products must be the activators of TRPV1 and TRPA1 channels in the incubated EGCG.   I further analyzed the sensitivity and selectivity to auto-oxidation products of four major catechins.   Catechins were dissolved and incubated for 3 hours, and then used to examine the activity to stimulate TRP channels. The activities were compared with the activities of catechins dissolved in 1 mM AA (Fig. 3 and 4).   EGCG and auto-oxidized EGCG were applied to cells at 2-200 μM, and then 10 μM capsaicin or 100 μM AITC was further applied to monitor the channel expression. Time courses of individual cell recordings are shown (Fig. 3A and 4A).   The average $[Ca^{2+}]_i$ response at 90 s with the 3 hours-incubated EGCG was obtained and plotted against the EGCG concentration (Fig. 3B and 4B).   In HEK293T cells expressing TRPV1, a significant increase in $[Ca^{2+}]_i$ was detected at 20 μM of the incubated EGCG.   In TRPA1-expressing HEK293T cells, a major response of $[Ca^{2+}]_i$ was observed from 100 μM. For other three major catechins (EC, ECG, EGC), the same experiments were performed

and results are summarized in Fig. 3B and 4B.   When compared among the four catechins, it is evident that the incubated EGCG most effectively induce the $[Ca^{2+}]_i$ spouse in HEK293T cells expressing TRPV1 or TRPA1.   Next, I examined whether blockers for TRP channels might block the increase in $[Ca^{2+}]_i$ induced with the EGCG.   A TRPA1-specific blocker, 4-(4-Chlorophenyl)-3- methylbut-3-en-2-oxime (AP-18), and a TRPV1-specific blocker, capsazepine (CPZ) were used.   I first examined the specificity of these blockers.   HEK293T cells were transfected with the expression vector for rat TRPV1, and cells were treated with 0.1 μM Capsaicin (CAP), 0.1 μM CAP and 10 μM CPZ, or 0.1 μM CAP and 100 μM AP-18 (Fig. 2A).   Analysis of calcium-imaging indicate that the CAP-induced activation of TRPV1 is significantly inhibited by 10 μM CPZ but not by 100 μM AP-18.   Similarly, HEK293T cells expressing mouse TRPA1 were treated with 10 μM AITC, 10 μM AITC and 10 μM CPZ or 10 μM AITC and 100 μM AP-18 (Fig. 2B), and calcium-imaging analysis was performed. Results showed that 100 μM AP-18 attenuated the AITC-induced activation of TRPA1, but 10 μM CPZ could not significantly reduced the activation.   Thus, I confirmed that CPZ and AP-18 selectively inhibit TRPV1 and TRPA1 cannels, respectively.

As indicated in Fig. 3C, 10 μM CPZ completely blocked the $[Ca^{2+}]_i$ spouse in HEK293T cells expressing TRPV1 induced with the auto-oxidized EGCG, but 100 μM AP-18 did not show a significant inhibitory effect.   Further, in TRPA1-expressing HEK293T cells, 100 μM AP-18 completely inhibited the increase in $[Ca^{2+}]_i$ with the auto-oxidized EGCG (Fig. 4C).   Thus, it is evident that the $[Ca^{2+}]_i$ responses induced by the incubated EGCG are mediated through specific TRP channel activation.

Sensitivity of DRG neurons to auto-oxidation products of EGCG

It has been known that the nerve fibers in the tongue express TRPV1 (Ishida et al., 2002), and it has been suggested that TRPA1-positive nerve fibers are present in the tongue (Nagatomo and Kubo, 2008). Primary afferent neurons are clustered in the dorsal root ganglion (DRG) and within cranial nerve ganglions such as the trigeminal ganglion (TG). It has been shown that DRG and TG neurons express TRPV1, TRPA1, and TRPM8 (Kobayashi et al, 2005). I wanted to know whether TRPV1 or TRPA1 channels in the nerves innervating the tongue are involved in the perception of the astringent taste of green tea. I examined the sensitivity of the acutely dissociated sensory DRG neurons to the auto-oxidized EGCG using the calcium-imaging technique. After the DRG was isolated from mice, neurons were dissociated and cultured.

After examining the specificity of anti-TRPV1 and anti-TRPA1 antibodies (fig. 5A), cultured mouse DRG neurons were immunostained with these antibodies. Most NF-positive neuron expressed TRPV1, and some NF-positive neurons did express TRPA1. Thus, TRPV1 and TRPA1 were expressed in mouse DRG neurons, and in some DRG neurons TRPV1 and TRPA1 were co-expressed in identical cells (fig. 5B). The expression of TRPV1 and TRPA1 in cultured DRG neuron was confirmed.

The freshly dissolved EGCG and the auto-oxidized EGCG were applied to DRG neurons at 200 μM. Time courses of individual cell recordings are shown in Fig. 6A. The mean maximum response in individual neurons during the first 120 s stimulation was compared with control. When the fresh EGCG was used, no significant increase in $[Ca^{2+}]_i$ was observed. On the other hand, auto-oxidized EGCG induce a $[Ca^{2+}]_i$ responses in DRG neurons. When EGCG was incubated in the presence of 1 mM AA, the increase in $[Ca^{2+}]_i$ was not induced by the EGCG. Further, the response of DRG neurons to the auto-oxidized EGCG was significantly attenuated with AP18 and CPZ (Fig. 6B). These results clearly

demonstrated that the responses to the auto-oxidized EGCG but not to EGCG itself were confirmed in DRG sensory neurons, and that they were mediated through TRPV1 and TRPA1 channels.

Preparation of an EGCG dimer, TS-A

Our results strongly demonstrated that EGCG was auto-oxidized during the 3 hours-incubation in HBSS buffer, and only the resultant products was active to stimulate TRPV1 and TRPA1 channels.   To study the changes in the EGCG solution, HPLC analysis was performed.   Fig. 7A shows the HPLC chromatogram of the freshly prepared EGCG.   A large peak with the retention time of 11.7 min corresponded to EGCG.   During the incubation for 3 hours in HBSS, several additional peaks appeared in addition to the peak of EGCG on the HPLC chromatogram.   High resolution (HR)-ESI/MS analysis demonstrated that two different EGCG dimers were present in the auto-oxidized products.   One peak with the retention time of 10.0 min showed a molecular ion of m/z 913.1492 (ESI negative, [M-H]$^{-}$).   Another peak with the retention time of 13.5 min also showed a molecular ion of m/z 913.1470 (ESI negative, [M-H]$^{-}$) (Fig. 7B).   Based on the calculate value ($C_{44}H_{33}O_{22}$ of 913.1463), the above two peaks were suggested to represent the isomeric dimers of EGCG, TS-A and TS-D. This was further confirmed by LC/MS/MS analysis.   The MS/MS spectra of their molecular ion [M-H]$^{-}$ Were consistent with those of the reported TS-A (591.2, 743.0, and 761.1, Hong et al., 2002; Sang et al., 2005).   LC/MS analysis further indicated that some dimers were also formed in the other major catechin in HBSS during 3 hours-incubation (Fig. 8).   The auto-oxidized products of EC, ECG, and EGC did not induce the high level of increase in $[Ca^{2+}]_i$ in the TRPV1 or TRPA1-expressing HEK293T cells (Fig. 3B and 4B).   Thus, it is possible that TSs present in the auto-oxidized products of EGCG might contribute to the activity to stimulate TRPV1 and TRPA1 channels.   To

examine this possibility, I decided to prepare TSs.　With the biomimetic method developed by Shii et al (2011), I synthesized and purified TS-A from EGCG (Fig. 9).　On the HPLC chromatogram of the purified product, one major peak with the retention time of 10.0 min was found.　HR-ESI/MS analysis showed a molecular ion of m/z 913.1414 (ESI negative, [M-H]$^-$), which is the same as the calculated for TS-A, $C_{44}H_{33}O_{22}$ (913.1463).　It was further confirmed by LC/MS/MS to be TS-A.　Namely, the MS/MS spectra were similar to the reported spectrum of TS-A showing mass fragments of 591.2, 743.0, and 761.1 (Hong et al., 2002; Sang et al., 2005).　Thus, I obtained highly pure TS-A.　In addition, I decided that on the HPLC chromatogram of the auto-oxidized EGCG, a peak with the retention time of 10.0 min in Fig. 7B contained TS-A and another peak with the retention time of 13.5 min in Fig. 7B corresponded to TS-D.

An EGCG dimer, TS-A activates TRPA1 and TRPV1 channels

I next examined how an EGCG dimer, TS-A acts on TRPA1 and TRPV1 channels. The expression vector of TRPA1 or TRPV1 was transfected into HEK293T cells and calcium-imaging analysis was performed using prepared TS-A (Fig. 10).　The increase in $[Ca^{2+}]_i$ was induced by TS-A in HEK293T cells expressing TRPV1 channels starting at 4 μM, and the response to TS-A increased up to 200 μM.　On the other hand, in case of TRPA1, the $[Ca^{2+}]_i$ spouse was first detected at 2 μM TS-A, a significant but slow increase in $[Ca^{2+}]_i$ was observed at 4 μM, and the response decreased at 40 μM and 200 μM.　The relationship between the average response at 90 s and the concentration of TS-A is shown. Results suggested that TS-A more efficiently stimulates TRPA1 than TRPV1.　I next examined whether blockers for TRP channels might block the increase in $[Ca^{2+}]_i$ induced with TS-A.　Although AP-18 had partial effect, CPZ completely inhibited the $[Ca^{2+}]_i$ spouse induced with TS-A in HEK293T cells expressing TRPV1.　Conversely, the

response in TRPA1-expressing HEK293T cells evoked by TS-A was completely blocked by AP-18.   CPZ partially attenuated the response.   These observations clearly demonstrate that EGCG itself cannot activate TRPV1 and TRPA1 channels, but that one of auto-oxidized products of EGCG, TS-A is indeed able to activate both TRP channels.

TS-A activates DRG neurons.

The prepared TS-A was applied to DRG neurons at 80 μM and calcium-imaging analysis was performed (Fig. 11).   Time courses of representative recordings were shown (Fig. 11A).   The average of highest response in individual neurons during the first 120 s stimulation was compared (Fig. 11B).   The increase in $[Ca^{2+}]_i$ in several DRG neurons was apparently observed with TS-A.   The response of DRG neurons to TS-A was significantly attenuated with AP-18 and CPZ.   These results strongly demonstrated that TS-A, which is formed in the course of auto-oxidation of EGCG, indeed activates DRG sensory neurons, and that this activation is mediated through TRPV1 and TRPA1 channels, providing an important information about the mechanism for astringent taste of food and beverages and one possible molecular explanation for sensing astringency of green tea after longer incubation.

Response of TRPV1 and TRPA1 channels from chick and snake.

Mammalian TRPV1 is activated by the pungent vanilloid capsaicin (Caterina et al., 1997).   On the other hand, it has been reported that a chick homolog of TRPV1 channel is insensitive to capsaicin (Jordt and Julius, 2002).   It has been shown that Mammalian TRPA1 channels are not activated by heat, but snake TRPA1 channels are heat-sensitive (Gracheva et al., 2010).   Thus, the diversity of channel properties among vertebrate TRPV1 and TRPA1 has been known (Nagatomo and Kubo, 2008; Gracheva et al., 2010; Saitoh et al., 2012).   Therefore, I decided to study whether TRPV1 and TRPA1 channels

from chick and snake might have sensitivity to the auto-oxidized EGCG.

Only the chick TRPA1 cDNA was not available.   To clone chick TRPA1 cDNA, RT-PCR was performed using total RNA from chick embryo DRG and the cDNA fragment containing the entire coding region of TRPA1 was amplified. The coding region of TRPA1 consisted of 3381 bp, resulting in 1126 amino acid residues (Fig. 12A and B).   chick TRPA1 exhibited 52.9%, 52.5%, 60.3%, 39.7%, and 36.6% amino acid sequence similarity to human TRPA1, mouse TRPA1, rattlesnake TRPA1, zebrafish TRPA1a, and zebrafish TRPA1b, respectively.

The expression vector for chick TRPV1, chick TRPA1, rattlesnake TRPV1, or rattlesnake TRPA1 was transfected into HEK293T cells and calcium-imaging analysis was performed (Fig. 12C).   The auto-oxidized products of major four catechins after 3 hours-incubation were used.   The increase in $[Ca^{2+}]_i$ was only observed in HEK293T cells expressing chick TRPV1.   Further, only the incubated EGCG induced a significant response.   Results suggested that the response to the oxidized catechins of TRP channels is species-specific sensitivity, and that birds and reptilians have limited sensitivity of the astringent taste of oxidized polyphenols from plants.

The region contributing to the TS-A sensitivity of TRPA1 channel

It is known that zebrafish TRPA1 paralogs (zTRPA1a and zTRPA1b), like mammalian TRPA1, can be activated by the pain-inducing natural products, AITC, cinnamaldehyde, and diallyl disulfide, by the environmental irritant acrolein, and by the endogenous compound 4-hydroxynonenal.   It was reported that a loss-of-function mutation in zTRPA1b reduced or abolished the robust increase in locomotors activity induced by these chemicals (Prober et al., 2008).   Oda et al. further reported that zTPA1a and zTRPA1b showed differential responses to chemical substances.   Namely, they demonstrated that zTRPA1a showed a

larger response or higher sensitivity to AITC, H_2O_2 and the oxidized EGCG than zTRPA1b (Oda, M. et al., 2013).   Therefore, I first studied whether zTRPA1 paralogs might have different sensitivity to the TS-A. HEK293T cells were transfected with the expression vector of zTRPA1a or zTRPA1b, calcium imaging analysis was performed using purified TS-A. We found that 4 μM TS-A activates zTRPA1a but not zTRPA1b (Fig.13B). Since zTRPA1a and zTRPA1b have a significant similarity (48.7%), I decided to investigate the region conferring the sensitivity to TS-A on zTRPA1a channel.   I focused on the ankyrin repeat (AR) domains and used chimeric ion channels between zTRPA1a and zTRPA1b (Oda, et al., 2013; Fig.13A).   When the B(10)A chimera was expressed in HEK293T cells, the $[Ca^{2+}]_i$ response was not induced with TS-A. But, when the B(5)A chimera was expressed, a significant elevation $[Ca^{2+}]_i$ was observed.   Treatment with 100 μM AITC induced the $[Ca^{2+}]_i$ response in HEK293T cells expressing zTRPA1 paralogs and the chimera channels. Namely, when AR 1-10 of zTRPA1a was exchanged for that of zTRPA1b, the sensitivity to TS-A of zTRPA1a was abolished.   But, when AR1-5 was exchanged, the TS-A sensitivity of zTRPA1a was not affected.   Result demonstrated that the region of AR 6-10 of zTRPA1a plays an important role for the response ability to TS-A.   Fig.13C indicates the amino acid alignment of the region of AR 6-10 of TRPA1 channels.   I searched amino acids, which are conserved among TS-A sensitive channels (hTRPA1, mTRPA1, zTRPA1a), but different in TS-A insensitive channels (cTRPA1, zTRPA1b).   Only two amino acids were found (indicated arrows).   These two amino acids may function as an essential binding site for TS-A.

Discussion

In this study, I examined how TRPA1 and TRPV1 are activated by tea catechins in the course of auto-oxidation process. Neither TRPA1 nor TRPV1 could be activated by any of the freshly prepared catechin, but the incubated and auto-oxidized EGCG significantly activated both TRP channels. Furthermore, I observed that DRG neurons are activated not by EGCG itself, but by the incubated EGCG through TRPV1 and TRPA1 channels. I analyzed the contents in the incubated auto-oxidized EGCG by LC/MS and found the presence of EGCG dimers, TSs. TS-A was prepared and the activity to stimulate TRP channels was studied. TS-A, which is one of the auto-oxidized products of EGCG, was shown to activate channels of TRPA1 and TRPV1. Further, TS-A activated DRG neurons by mediating through TRPV1 and TRPA1. TRPV1 is expressed in the nerves innervating the tongue (Ishida et al., 2002), and TRPA1 is also suggested to be expressed in nerves on the tongue (Nagatomo and Kubo, 2008). These findings provided insights into the mechanism for astringent taste of polyphenol-containing foods and beverages on the tongue.

Auto-oxidized products of EGCG other than TS-A

When the incubated EGCG was applied to HEK293T cells expressing TRPA1, a significant increase in $[Ca^{2+}]_i$ was observed starting at 100 μM (Fig. 4B). When purified TS-A was used, the $[Ca^{2+}]_i$ spouse was first detected at 2 μM and significantly induced at 4 μM (Fig. 10B). These results indicated that TS-A is one of the oxidized products which are formed during the 3 hours-incubation and selectively activates TRPA1 channels. In case of TRPV1, 20 μM of the oxidized EGCG induced an apparent increase in $[Ca^{2+}]_i$ and the decreased response was observed with 200 μM of the EGCG in TRPV1-expressing HEK293T cells (Fig. 3B). On the other hand, purified TS-A can induce the $[Ca^{2+}]_i$ spouse in TRPV1-expressing HEK293T cells, but the high level response was only induced with 200

μM TS-A (Fig. 10B). Thus, the sensitivity of TRPV1 to TS-A was not so high. These observations suggested that some oxidized products other than TS-A might be present in the EGCG solution incubated for 3 h, and that they might specifically stimulate TRPV1 channels. Although further investigation is required, TS-D, another dimer of EGCG, might be a candidate.

Cross-talk between TRPV1 and TRPA1.

AP-18 specifically and completely inhibited the channel activation in HEK293T cells expressing TRPA1, and CPZ specifically and completely inhibited the channel activation in HEK293T cells expressing TRPV1. In DRG neuron, there are TRPV1- and TRPA1-expressing neurons, TRPV1- and TRPM8-expressing neurons, and TRPA1 and TRPM8-expressing neurons (Kobayashi et al., 2005). In the presence of a TRPA1 channel-specific blocker, it was expected that neurons of DRG expressing TRPV1 still might be able to respond to the auto-oxidized EGCG or TS-A. However, when DRG neurons were treated with a TRPA1 channel-specific blocker, AP-18, cellular response induced with the auto-oxidized EGCG or TS-A was greatly inhibited (Fig. 6 and Fig. 11). It has been demonstrated that TRPV1 and TRPA1 channels assemble into a complex on the plasma membrane, and that they mutually control the transduction of inflammation-induced noxious stimuli in sensory neuron (Akopian et al., 2007; Akopian et al., 2008; Staruschenko et al., 2010). Therefore, by interaction between TRPA1 and TRPV1 channels, it seems that the treatment with AP-18 might indirectly attenuate TRPV1 channels in DRG neurons simultaneously expressing TRPA1, and that a TRPV1 blocker, CPZ might function similarly on TRPV1 and TRPA1 channels.

The mechanism to activate TRPV1 and TRPA1 with auto-oxidized EGCG.

When the time courses of individual cell recordings of TRPV1-expressing and

TRPA1-expressing HEK293T cells were compared (Fig. 3A, 4A, and Fig. 10), the level of $[Ca^{2+}]_i$ rather gradually increased sometimes with some delay in the TRPA1-expressing cells after application of the oxidized EGCG or TS-A.   In HEK293T cells expressing TRPV1, the relatively rapid increase in $[Ca^{2+}]_i$ was observed with the oxidized EGCG or TS-A.   It seems that there might be different mechanism to activate TRPV1 and TRPA1 channels.   It has been reported for human TRPA1 that 15-deoxy-$\Delta^{12, 14}$-prostaglandin J_2 induces rapid activation, but NO and H_2O_2 activate channels with a time-lag after application.   It has been suggested that those channel activations might be mediated through differential modification of cysteine residues in the cytoplasmic N-terminus of TRPA1 by these inflammatory mediators (Andersson et al., 2008; Sawada et al., 2008; Takahashi et al., 2008).   Further, it has been shown that the treatment with H_2O_2 sensitizes TRPV1 channels through modification of multiple cysteine residues present in TRPV1 proteins (Chuang and Lin, 2009). It is possible that the oxidized EGCG products might modify or binding to specific residues to activate TRPV1 or TRPA1 channels.   To approach the molecular mechanism to activate these TRP channels by the oxidized EGCG and TS-A, further investigation using chimeras between the oxidized EGCG-sensitive and insensitive TRP channels are important.

Figure Legends

Fig. 1 Auto-oxidized EGCG stimulates rat TRPV1 and mouse TRPA1 channels.

(A) Effects of freshly prepared and incubated epigallocatechin gallate (EGCG, 200 μM) on $[Ca^{2+}]_i$ in HEK293T cells expressing rat TRPV1 were examined.   After transfection with the expression vector of rat TRPV1, cells were loaded with 5 μM Fluo8-AM.   The Fluo8 fluorescence was recorded every 3 s and the relative fluorescent change (ΔF/F) was determined.   At 6 s, EGCG (fresh or incubated) was applied.   At 240 s, 10 μM capsaicin (CAP) was further applied to confirm the channel expression.   200 μM EGCG in HBSS was freshly prepared (0 h), or prepared and incubated at $25^{o}C$ for 2 hours (2 h), 4 hour (4 h), 6 hours (6 h).   200 μM EGCG in HBSS containing 1mM AA was prepared and incubated at $25^{o}C$ for 2 hours (EGCG+AA).   HBSS containing 1 mM AA without EGCG was also prepared. They were used as a ligand solution.   The average ΔF/F at 90 s was obtained and compared.   Differences were judged to be significant by the Tukey-Kramer method (**$p < 0.01$).   Result of 0h EGCG was significantly different from result of 2 h EGCG (**). Results of 2h EGCG and EGCG+AA were significantly different (**).

(B) Effects of freshly prepared and incubated 200 μM EGCG on $[Ca^{2+}]_i$ in HEK293T cells expressing mouse TRPA1 were examined.   After transfection with the expression vector of mouse TRPA1, calcium-imaging analysis was similarly performed as A.   At 6 s, EGCG (fresh or incubated) was applied.   At 240 s, 100 μM AITC was further applied to monitor the channel expression.   The same set of ligand solutions as A was used.   The average ΔF/F at 90 s was obtained and compared.   Differences were judged to be significant by the Tukey-Kramer method (**$p < 0.01$).   Result of 0h EGCG was significantly different from result of 2h EGCG (**).   Results of 2 h EGCG and EGCG+AA were significantly different (**).

Fig. 2 Effect of antagonists on the capsaicin-response of TRPV1 and the AITC-response of TRPA1.

Effects of channel blockers on the Ca^{2+} response in rat TRPV1-expressing or mouse TRPA1-expressing cells induced by CAP or AITC, respectively were examined.   The average $\Delta F/F$ at 27 s was obtained and compared.   Differences were judged to be significant by the Tukey-Kramer method (**$p<0.01$).

(A) To HEK293T cells expressing rat TRPV1, 0.1 μM CAP was singly, with 10 μM CPZ, or with 100 μM AP-18 applied to cells at 6 s.   Results of 0.1 μM CAP and CAP+CPZ were significantly different (**).

(B) To HEK293T cells expressing mouse TRPA1, 10 μM AITC was singly, with 10 μM CPZ, or with 100 μM AP-18 applied to cells at 6 s. Results of AITC and AITC+AP-18 were significantly different (**).

Fig. 3 Effects of the incubated catechins on rat TRPV1 channels.

(A) Effects of EGCG or incubated EGCG on $[Ca^{2+}]_i$ in HEK293T cells expressing rat TRPV1 were examined.   HEK293T cells expressing rat TRPV1 were loaded with 5 μM Fluo8-AM.   The Fluo8 fluorescence was recorded every 3 s and $\Delta F/F$ was determined.   At 6 s, ligand was applied.   At 120 s, 10 μM CAP was further applied to monitor the channel expression. EGCG was prepared in HBSS containing 1 mM AA (EGCG), or prepared in HBSS without 1mM AA and incubated at $25^{o}C$ for 3 hours (3 h EGCG).   They were used as a ligand solution.   Time courses of $\Delta F/F$ of individual cell recordings were shown.

(B) Effects of catechins or incubated catechins on $[Ca^{2+}]_i$ in HEK293T cells expressing rat TRPV1 were examined.   The calcium-imaging analysis of HEK293T cells expressing rat TRPV1 was similarly performed as in A, except for ligand solutions.   Epicatechin (EC), epigallocatechin (EGC), epicatechin gallate (ECG) or EGCG was prepared in HBSS

containing 1mM AA (left), or prepared in HBSS without 1mM AA and incubated at 25°C for 3 hours (right). They were used as a ligand solution. The average $\Delta F/F$ at 90 s was obtained and plotted against the catechin concentration. Differences were judged to be significant by the Tukey-Kramer method (*$p<0.05$, **$p<0.01$). Result of 20 μM EGCG was significantly different from result of 20 μM EGC (**) and from result of 20 μM EC (**). Results of 20 μM EGCG and 20 μM ECG were significantly different (*).

(C) The calcium-imaging analysis of HEK293T cells expressing rat TRPV1 was performed, and effects of channel blockers on TRPV1 activation induced by the incubated EGCG were examined. 20 μM EGCG was prepared in HBSS and incubated at 25°C for 3 hours. This 20 μM EGCG was singly, with 100 μM AP-18, or with 10 μM CPZ applied to cells at 6 s. The average $\Delta F/F$ at 90 s was obtained and compared. Differences were judged to be significant by the Tukey-Kramer method (**$p<0.01$). Results of 20 μM EGCG and 20 μM EGCG+CPZ were significantly different (**).

Fig. 4 Effects of the incubated catechins on mouse TRPA1 channels.

(A) Effects of EGCG or incubated EGCG on $[Ca^{2+}]_i$ in HEK293T cells expressing mouse TRPA1 were examined. The calcium-imaging analysis of HEK293T cells expressing mouse TRPA1 was performed and $\Delta F/F$ was determined. At 6 s, ligand was applied. At 120 s, 100 μM AITC was further applied. EGCG was prepared in HBSS containing 1 mM AA (EGCG), or prepared in HBSS without 1 mM AA and incubated at 25°C for 3 hours (3 h EGCG). They were used as a ligand solution. Time courses of $\Delta F/F$ of individual cell recordings were shown.

(B) Effects of catechins or incubated catechins on $[Ca^{2+}]_i$ in HEK293T cells expressing mouse TRPA1 were examined. The calcium-imaging analysis of HEK293T cells expressing mouse TRPA1 was performed. EC, EGC, ECG or EGCG was prepared in HBSS containing 1 mM

AA (left), or prepared in HBSS without 1 mM AA and incubated at 25°C for 3 hours (right). They were used as a ligand solution. The average ΔF/F at 90 s was obtained and plotted against the catechin concentration. Differences were judged to be significant by the Tukey-Kramer method (**p<0.01). Result of 100 μM EGCG was significantly different from result of 100 μM EGC (**), from result of 100 μM EC (**), and from result of 100 μM ECG (**).

(C) The calcium-imaging analysis of HEK293T cells expressing mouse TRPA1 was performed, and effects of channel blockers on TRPA1 activation induced by the incubated EGCG were examined. 100 μM EGCG was prepared in HBSS and incubated at 25°C for 3 hours. This 100 μM EGCG was applied alone, with 100 μM AP-18, or with 10 μM CPZ to cells at 6 s. The average ΔF/F at 90 s was obtained and compared. Differences were judged to be significant by the Tukey-Kramer method (**p<0.01). Results of 100 μM EGCG and 100 μM EGCG+AP-18 were significantly different (**).

Fig. 5 The expression of TRPV1 and TRPA1 in mouse DRG.

(A) The expression vector of rat TRPV1 or mouse TRPA1 was transfected into HEK293T cells. At 24-48 h after transfection, cells were fixed and permeabilized with 0.5% Triton X-100. Then, cells were immunostained with anti-TRPV1 or anti-TRPA1 antibody. Immunoreation was visualized with Alexa488 labelled 2nd antibody.

Positive staining with each antibody was seen in cells transfected with rat TRPV1 cDNA (b) or with mouse TRPA1 cDNA (d), but no apparent signed was detected in non-transfected cells with either antibodies (f and h). Phase-contrast and corresponding immune-fluorescent images were indicated (a, c, e and h). Scale bar, 20 μm.

(B) Cultured mouse DRG cells were fixed and permeabilized with 0.5% Triton X-100. Then DRG cells were doubly immunostained using anti-NF antibody (b) and anti-TRPV1

antibody (c), or anti-NF antibody (e) and anti-TRPA1 antibody (f).   Immunoreaction with anti-NF was detected with alexa 568 labelled 2nd antibodies.   Signals with anti-TRPV1 antibody or anti-TRPA1 antibody were visualized with Alexa 488 2nd antibody. Phase-contrast and corresponding immunofluorecent images were shown (a and d).   Scale bar, 20 μm.

Fig. 6 Effects of the incubated EGCG on mouse DRG neurons.

(A) Ca^{2+} response of DRG neurons to the incubated EGCG was examined.   DRG sensory neurons were isolated from mice and cultured.   On culture day 1, the calcium-imaging analysis was performed.   200 μM EGCG in HBSS was freshly prepared (0 h EGCG), or prepared and incubated at 25°C for 3 hours (3 h EGCG).   200 μM EGCG in HBSS containing 1 mM AA was prepared and incubated at 25°C for 3 hours (3 h EGCG (+AA)).   3 h EGCG was mixed with 100 μM AP-18, or with 10 μM CPZ.   They were used as a ligand solution at 6 s, 100 μM AITC was applied at 120 s, and 10 μM CAP was further applied at 150 s.   Time courses of ΔF/F of individual cell recordings were shown.

(B) From results in (A), the average of the highest response in individual neurons during the first 120 s stimulation was obtained and compared.   Differences were judged to be significant by the Tukey-Kramer method (**p<0.01).   Results of 0 h EGCG and 3 h EGCG were significantly different (**).   Result of 3 h EGCG was significantly different from result of 3 h EGCG (+AA) (**), from result of 3 h EGCG+AP-18 (**), and from result of 3 h EGCG+CPZ (**).

Fig. 7 Identification of EGCG dimmers in the EGCG incubated for 3 h.

(A) Liquid chromatography (LC) of EGCG.   4 mM EGCG was dissolved in HBSS containing 1 mM AA and analyzed by HPLC.

(B) LC, MS, and MS/MS spectra of the incubated EGCG.   4 mM EGCG was dissolved in

HBSS, incubated for 3 hours, and analyzed by LC/MS/MS.　ESI negative MS and MS/MS spectra of one major peak (T_R 10.0) were shown in left.　The peak with T_R 10.0 showed a major molecular ion of m/z 913.1492.　ESI negative MS and MS/MS spectra of another major peak (T_R 13.5) were shown in right.　The peak with T_R 13.5 showed a major molecular ion of m/z 913.1470. Calculated exact mass of TS-A and TS-D is 913.1463.　These two peaks contained TS-A and TS-D, isomeric dimers of EGCG.

Fig. 8 LC and LC/MS analysis of the incubated EC, ECG, and EGC.

(A) Liquid chromatography (LC) of EC (MW 290.27) was shown in upper panel.　4 mM EC was dissolved in HBSS containing 1mM AA and analyzed by HPLC.　One major peak (*0) is EC.　LC and MS spectra of the incubated EC were shown in lower panels.　4 mM EC was dissolved in HBSS, incubated for 3 hours, and analyzed by LC/MS.　ESI negative MS spectra of one peak (*1, T_R 12.5) were shown in right.　The peak with T_R 12.5 showed a major molecular ion of m/z 577.1278.

(B) LC of ECG (MW 442.37) was shown in upper panel.　4 mM ECG was dissolved in HBSS containing 1 mM AA and analyzed by HPLC.　One major peak (*0) is ECG.　LC and MS spectra of the incubated ECG were shown in lower panels.　4 mM ECG was dissolved in HBSS, incubated for 3 hours, and analyzed by LC/MS.　ESI negative MS spectra of one peak (*1, T_R 20.6) were shown in right.　The peak with T_R 20.6 showed a major molecular ion of m/z 881.1217.

(C) LC of EGC (MW 306.27) was shown in upper panel.　4 mM EGC was dissolved in HBSS containing 1 mM AA and analyzed by HPLC.　One major peak (*0) is EGC.　LC and MS spectra of the incubated EGC were shown in lower panels.　4 mM EGC was dissolved in HBSS, incubated for 3hours, and analyzed by LC/MS.　ESI negative MS spectra of one peak (*1, T_R 20.3) were shown in right.　The peak with T_R 20.3 showed a major molecular ion of

m/z 607.0828.   A molecular ion of m/z 520.8881 was from background, since it was always

detected.

Fig. 9 Preparation of TS-A.

As described in Materials and Methods section, TS-A was synthesized and purified according

to the method of Shii et al (2011).   The main peak from the preparative HPLC of the reaction

mixture was analyzed by LC/MS/MS.   ESI negative MS and MS/MS spectra of the main

peak (T_R 10.0) were shown in right.   The peak with T_R 10.0 showed a major molecular ion of

m/z 913.1414.   Calculated exact mass of TS-A is 913.1463.

Fig. 10 TS-A stimulates rat TRPV1 and mouse TRPA1 channels.

(A) Effects of prepared TS-A on $[Ca^{2+}]_i$ in HEK293T cells expressing rat TRPV1 or mouse

TRPA1 were examined.   After transfection with the expression vector (rat TRPV1 or mouse

TRPA1), the calcium-imaging analysis was performed, then ΔF/F was determined.   At 6 s,

TS-A (2 μM, 4 μM, 40 μM, and 200 μM) was applied.   At 120 s, 10 μM CAP or 100 μM

AITC was further applied to confirm the channel expression.   Time courses of ΔF/F of

individual cell recordings were shown.

(B) From results described A, the average ΔF/F at 90 s was obtained and plotted against the

concentration of TS-A.

(C) Effects of channel blockers on the Ca^{2+} response in rat TRPV1-expressing or mouse

TRPA1-expressing cells induced by TS-A.   To HEK293T cells expressing rat TRPV1, 200

μM TS-A was singly, with 100 μM AP-18, or with 10 μM CPZ applied to cells at 6 s.   The

average ΔF/F at 90 s was obtained and compared (left).   To HEK293T cells expressing rat

TRPA1, 40 μM TS-A was singly, with 100 μM AP-18, or with 10 μM CPZ applied to cells at

6 s.   The average ΔF/F at 90 s was obtained and compared (right). Differences were judged

to be significant by the Tukey-Kramer method (**$p < 0.01$).   For rat TRPV1-expressing cells,

results of 200 μM TS-A and 200 μM TS-A+CPZ were significantly different (**).   For mouse TRPA1-expressing cells, results of 40 μM TS-A and 40 μM TS-A+AP-18 were significantly different (**).

Fig. 11 TS-A stimulates mouse DRG neurons.

(A) Effects of prepared TS-A on $[Ca^{2+}]_i$ in DRG neurons were examined by the calcium-imaging analysis.   At 6 s, 80 μM TS-A was singly, with 100 μM AP-18, or with 10 applied at 150 s.   Time courses of ΔF/F of individual cell recordings were shown.

(B) From results in A, the average of the highest response in individual neurons during the first 120 s stimulation was obtained and compared.   Differences were judged to be significant by the Tukey-Kramer method (*$p<0.05$, **$p<0.01$).   Results of TS-A and TS-A+AP-18 was significantly different (*).   Result of TS-A was significantly different from result of TS-A+CPZ (**).

Fig. 12 The incubated EGCG activates chick TRPV1 but not chick TRPA1.

(A) Nucleotide sequence of chick TRPA1 cDNA.

(B) Deduced amino acid sequence of chick TRPA1

(C) Effects of incubated catechins on $[Ca^{2+}]_i$ in HEK293T cells expressing chick TRPV1, chick TRPA1, rattlesnake TRPV1, and rattlesnake TRPA1 were examined.   After transfection with the expression vector, calcium-imaging analysis was performed.   EC, EGC, ECG, or EGCG was prepared in HBSS and incubated at 25°C for 3 h.   They were used as a ligand solution at 6 s.   The average ΔF/F at 90 s was obtained and plotted against the catechin concentration.   Only chick TRPV1 channels were activated with the incubated EGCG.   Differences were judged to be significant by the Tukey-Kramer method (**$p<0.01$). For chick TRPV1, result of 200 μM EGCG was significantly different from result of 200 μM EGC (**), from result of 200 μM ECG (**), and from result of 200 μM EC (**).

Fig. 13 Search for the putative TS-A-binding site in zebrafish TRPA1a channel.

(A) Schematic representation of zTRPA1a, zTRPA1b, and zTRPA1a-zTRPA1b chimeras are shown. AR: ankyrin repeat; TM: Transmembrane domain.

(B) Response of zTRPA1a, zTRPA1b, and zTRPA1a-zTRPA1b chimeras to TS-A were examined. After transfection with the expression vector (zTRPA1a, zTRPA1b, B(10)A, B(5)A), the calcium-imaging analysis was performed and $\Delta F/F$ was determined. At 6 s, 4 µM TS-A was applied. At 120 s, 100 µM AITC was further applied to confirm the channel expression. The average $\Delta F/F$ at 90 s was obtained and compared. Differences were judged to be significant by the Tukey-Kramer method (**$p<0.01$). The chimera B(5)A contains a minimal segment of zTRPA1a that is sufficient to confer TS-A sensitivity. Result of zTRPA1a was significantly different from result of zTRPA1b (**) and from result of B(10)A (**). Result of B(5)A was significantly different from result of zTRPA1b (**) and from result of B(10)A (**).

(C) The sequence alignment of the ankyrin repeats 5-10 of TRPA1channels of human, mouse, chick, zebrafish is shown. Conserved residues are indicated by asterisks (*). The amino acid, which is conserved among human, mouse, and zTRPA1a but specific for chick or zTRPA1b, is indicated by arrows.

Figure 1

Figure 2
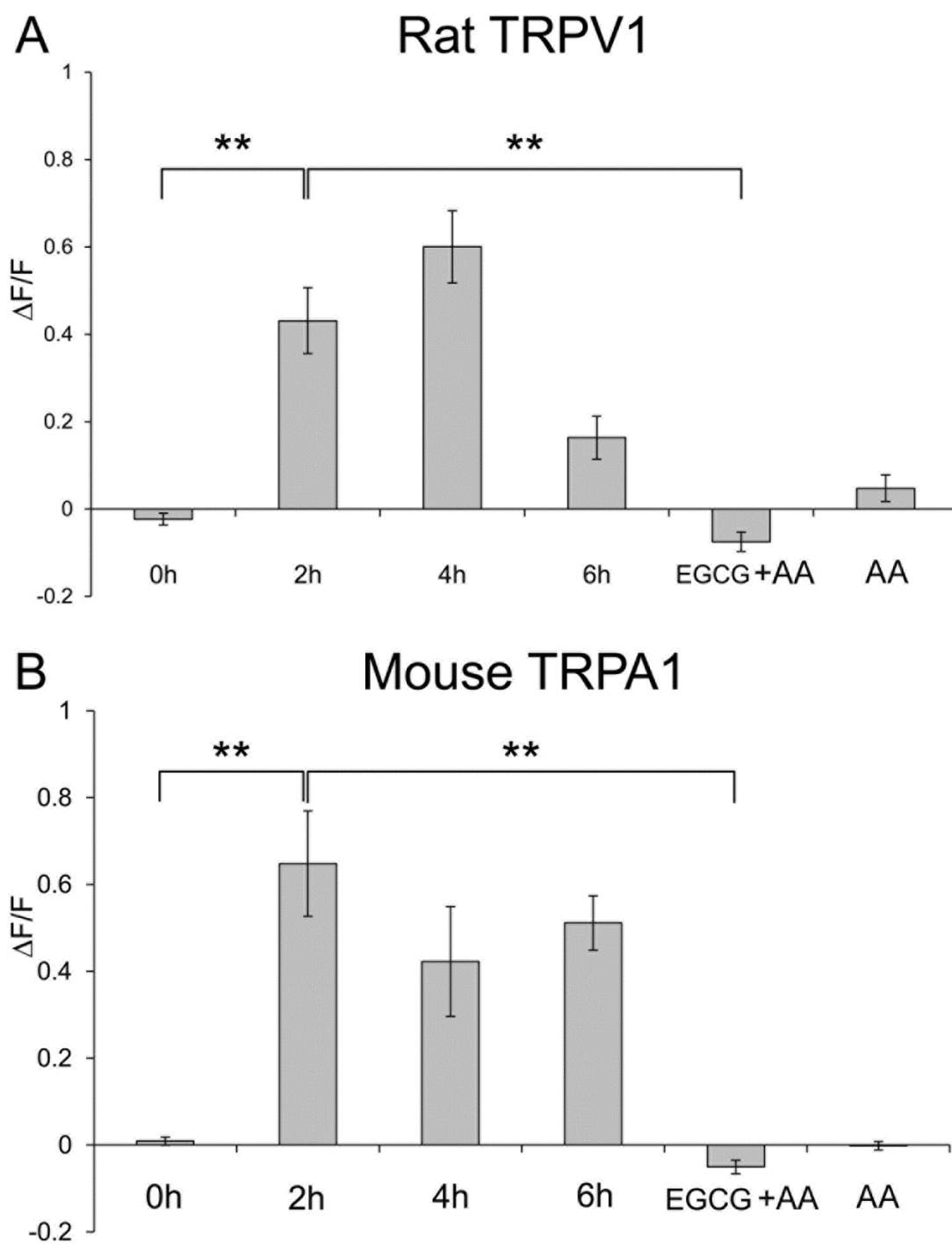
A Rat TRPV1
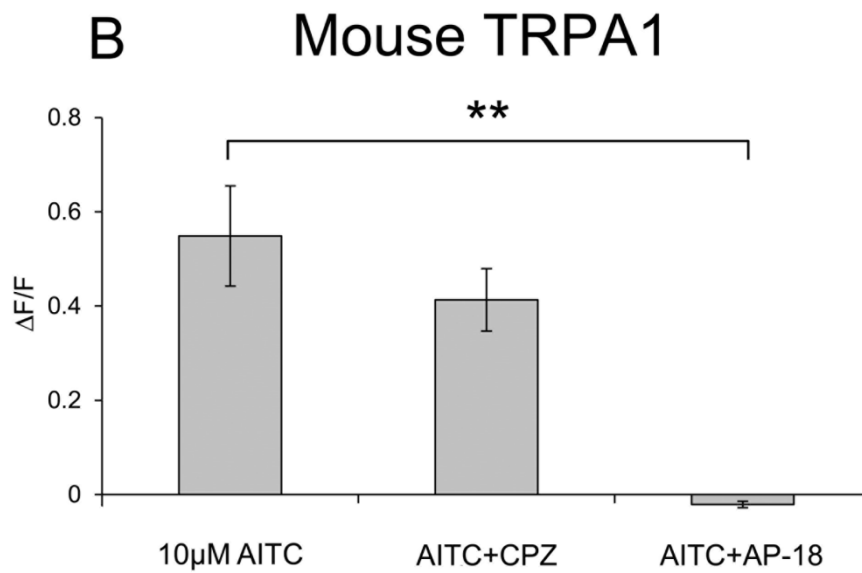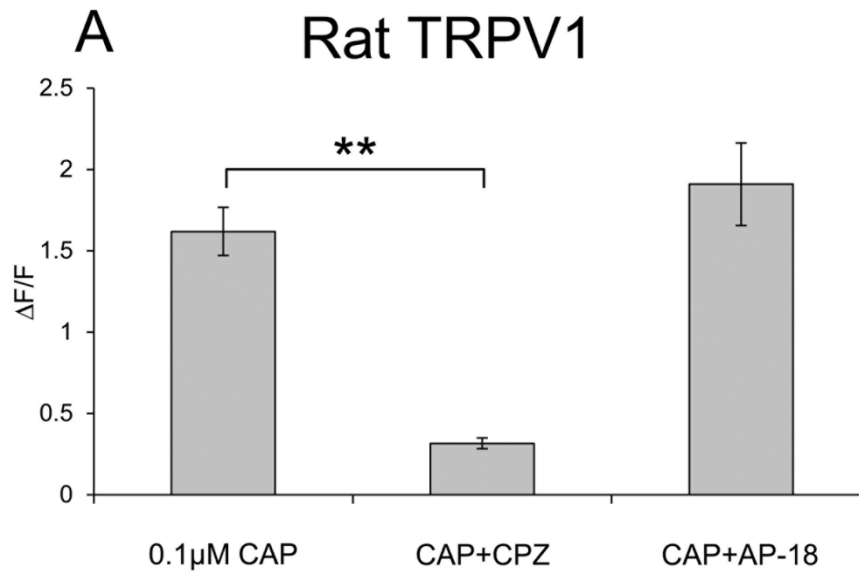
B Mouse TRPA1

Figure 3

Rat TRPV1
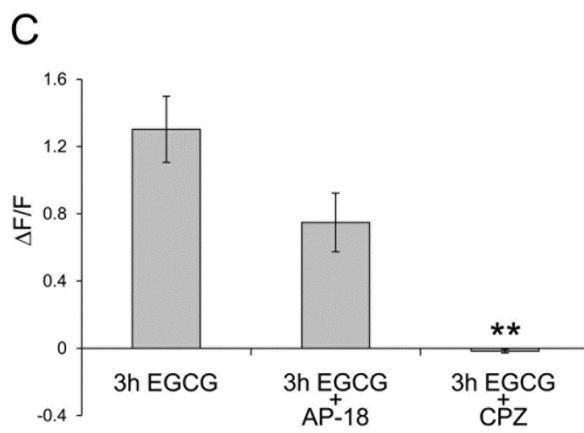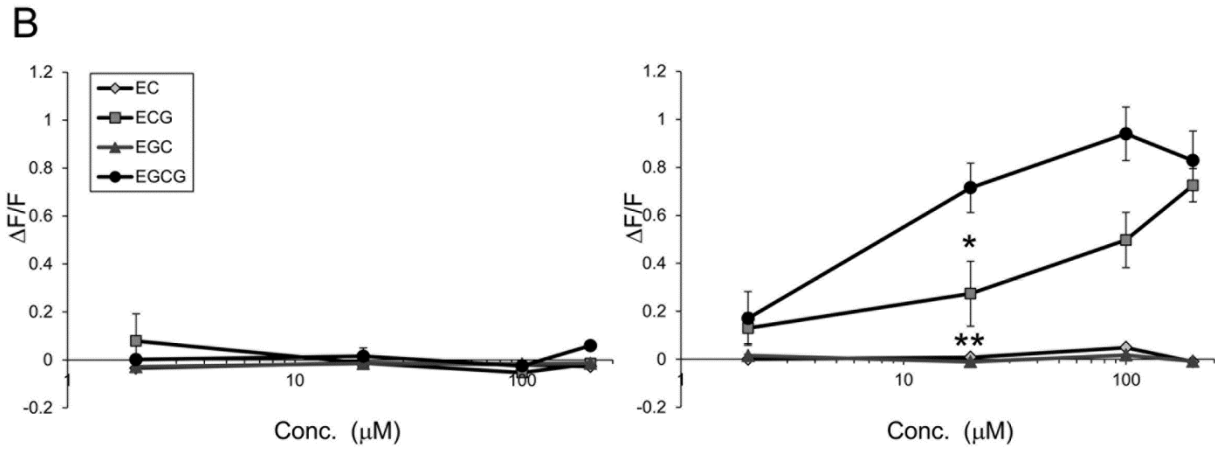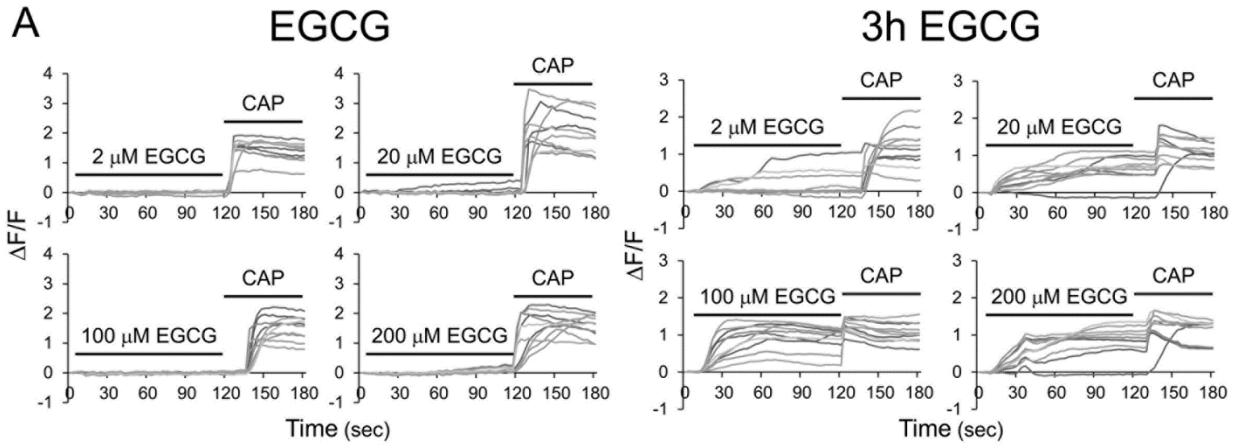
Figure 4

Mouse TRPA1
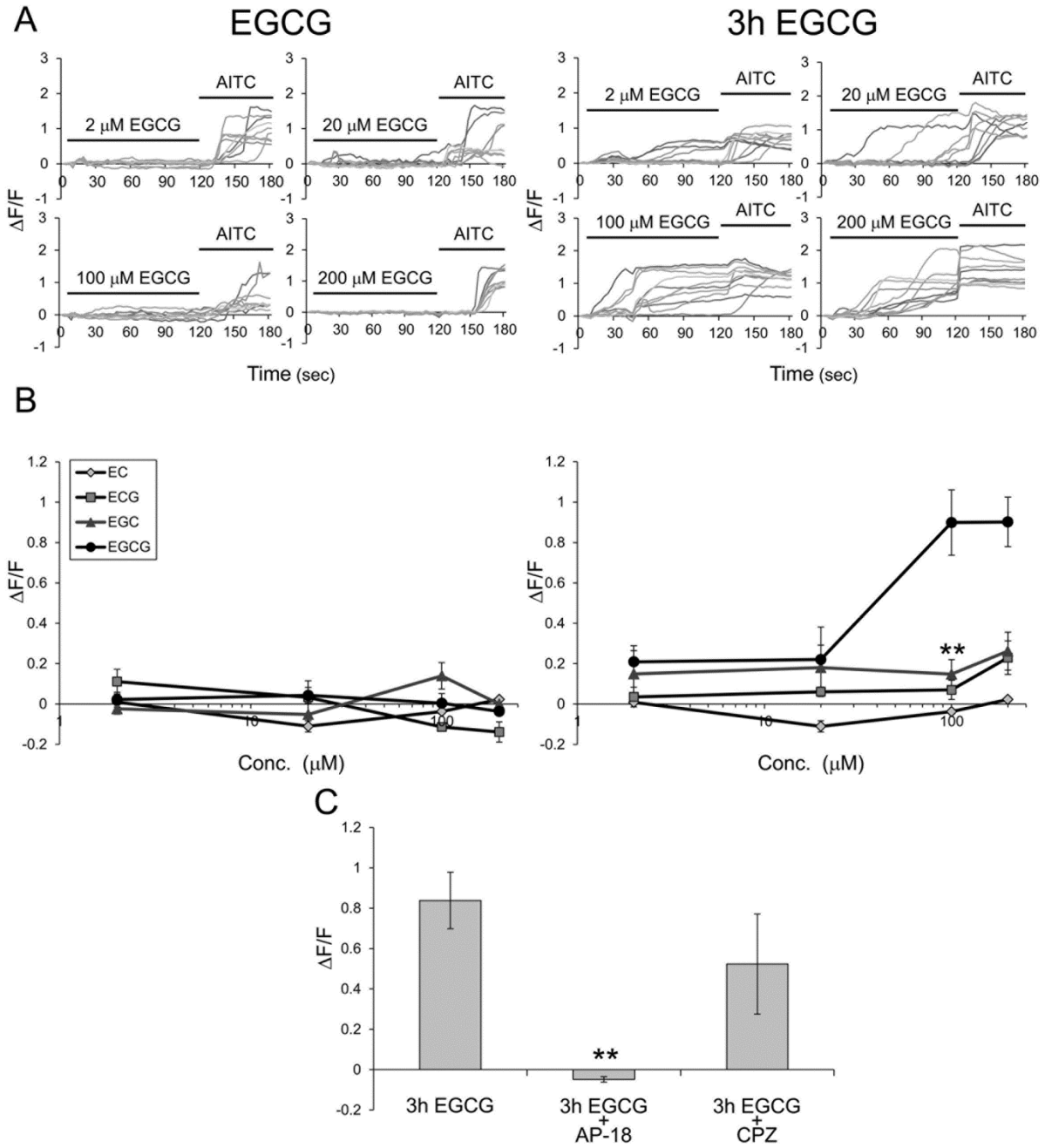
Figure 5
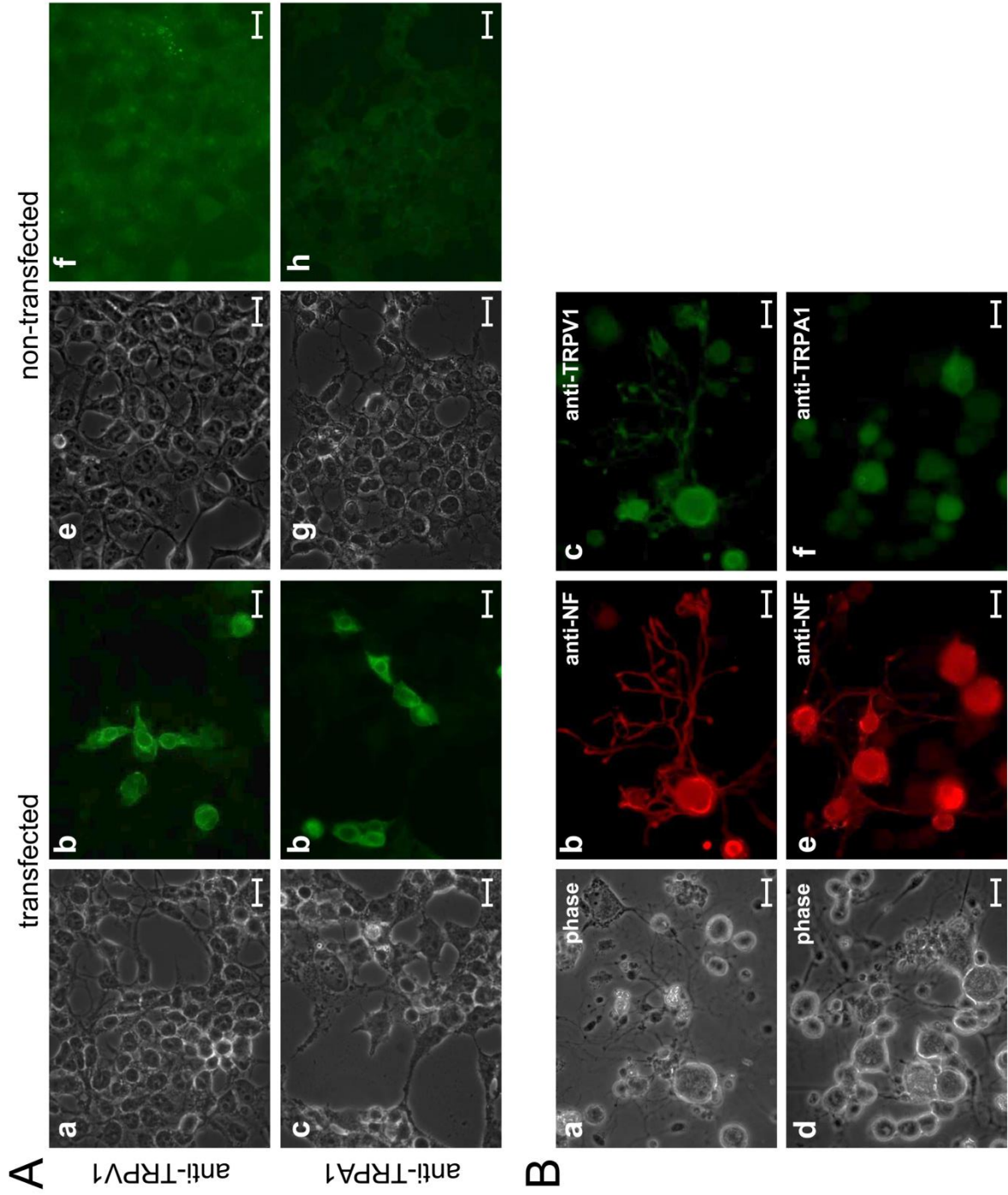
Figure 6
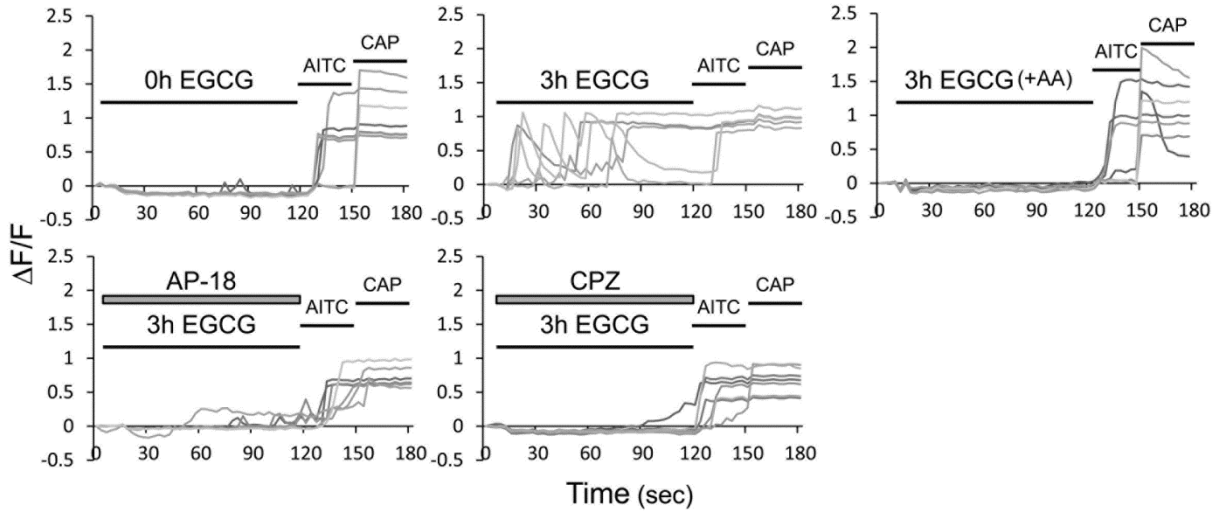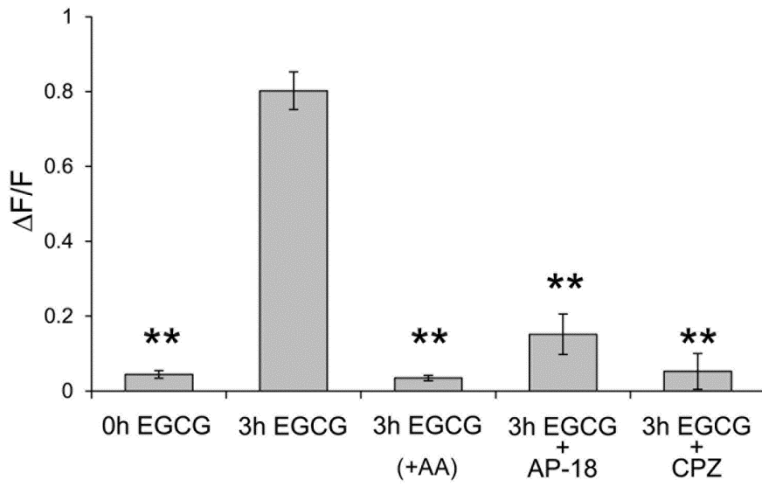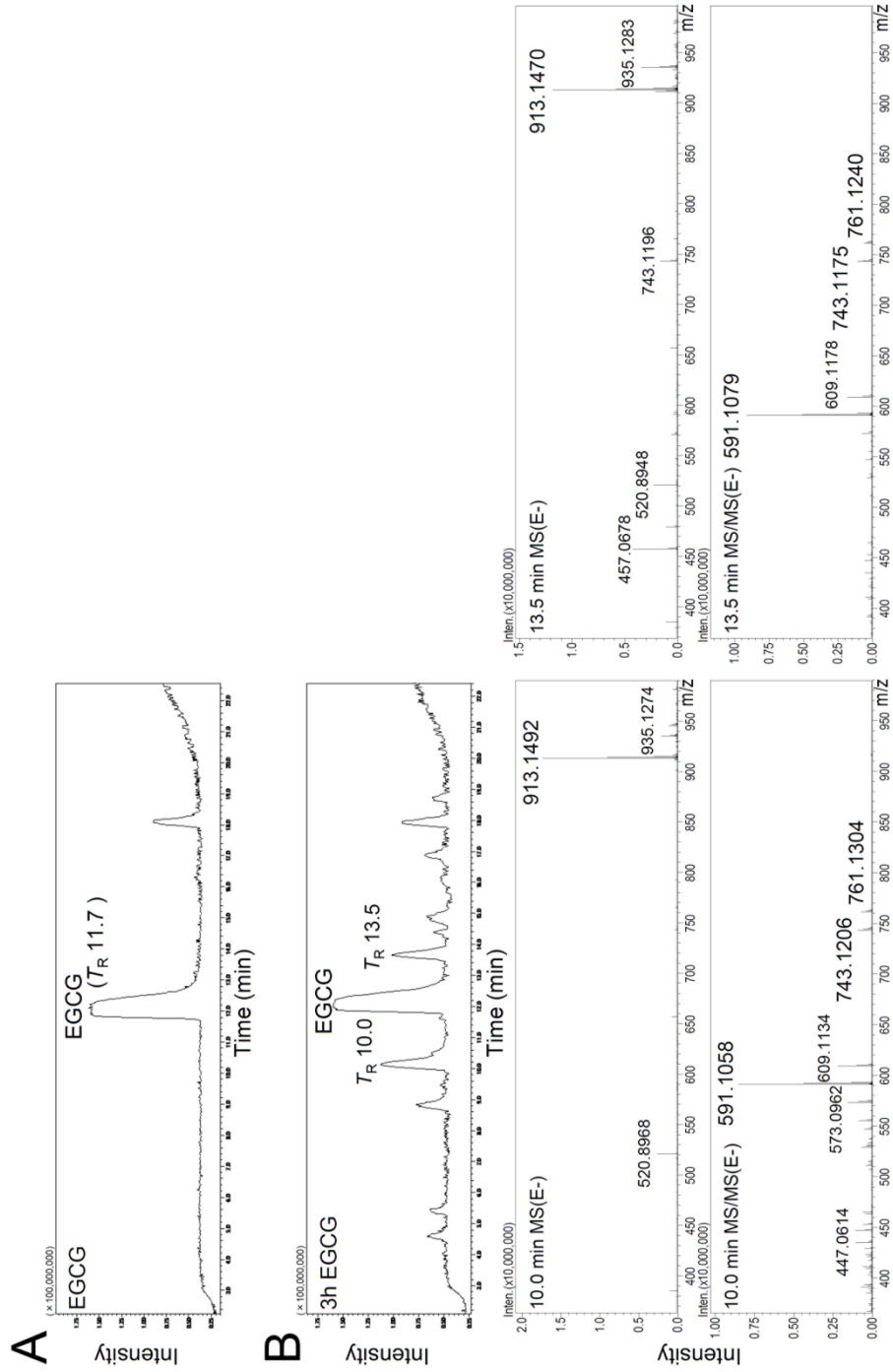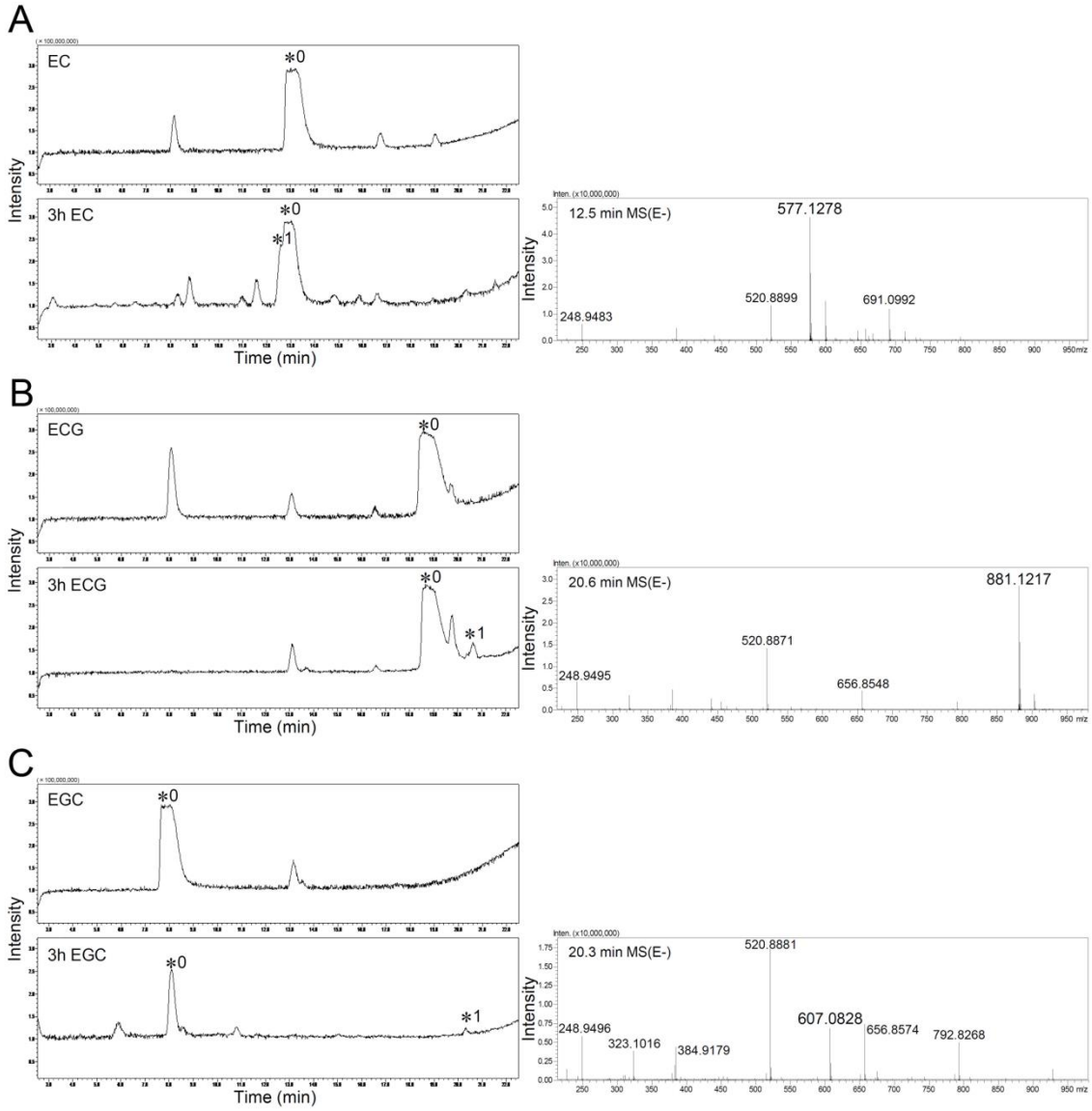
Figure 7

Figure 8

Figure 9
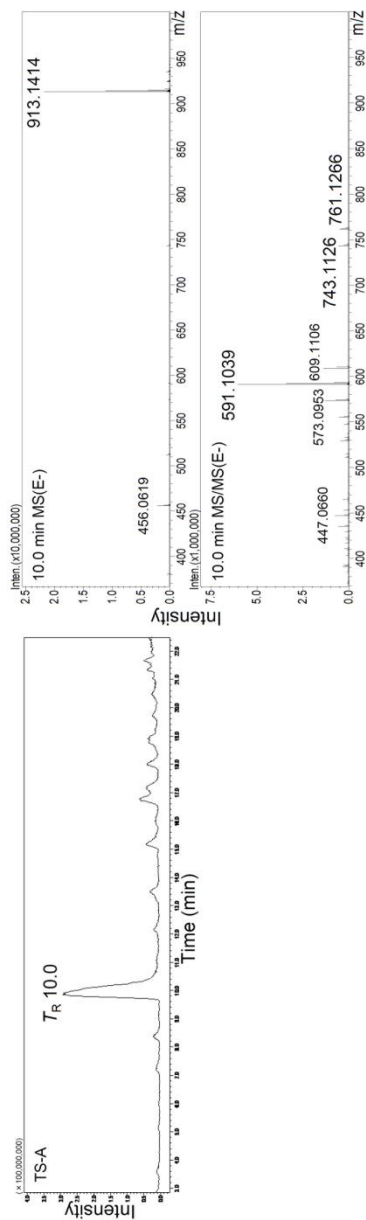
Figure 10
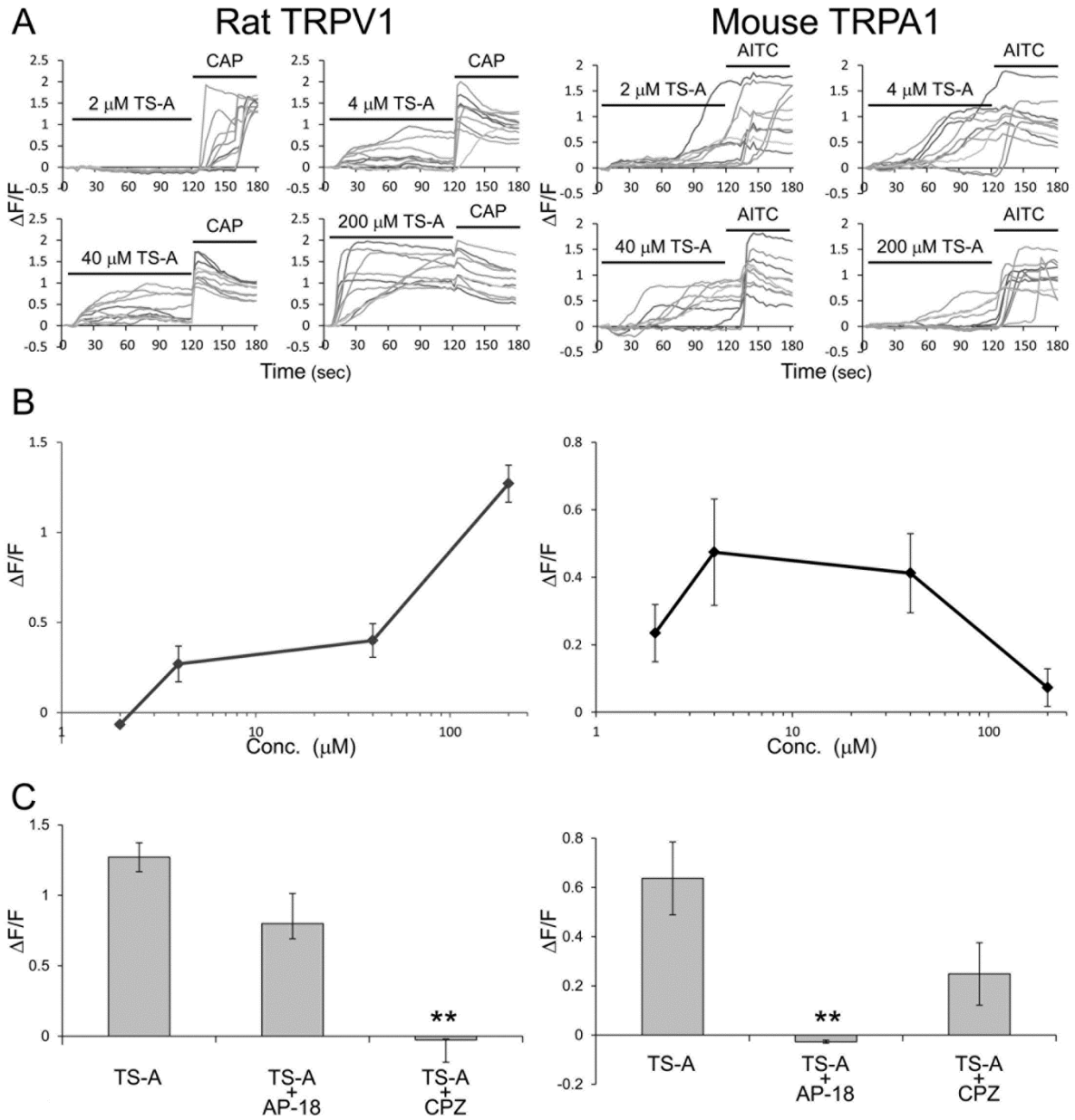
Figure 11

Figure 12

A

B

C
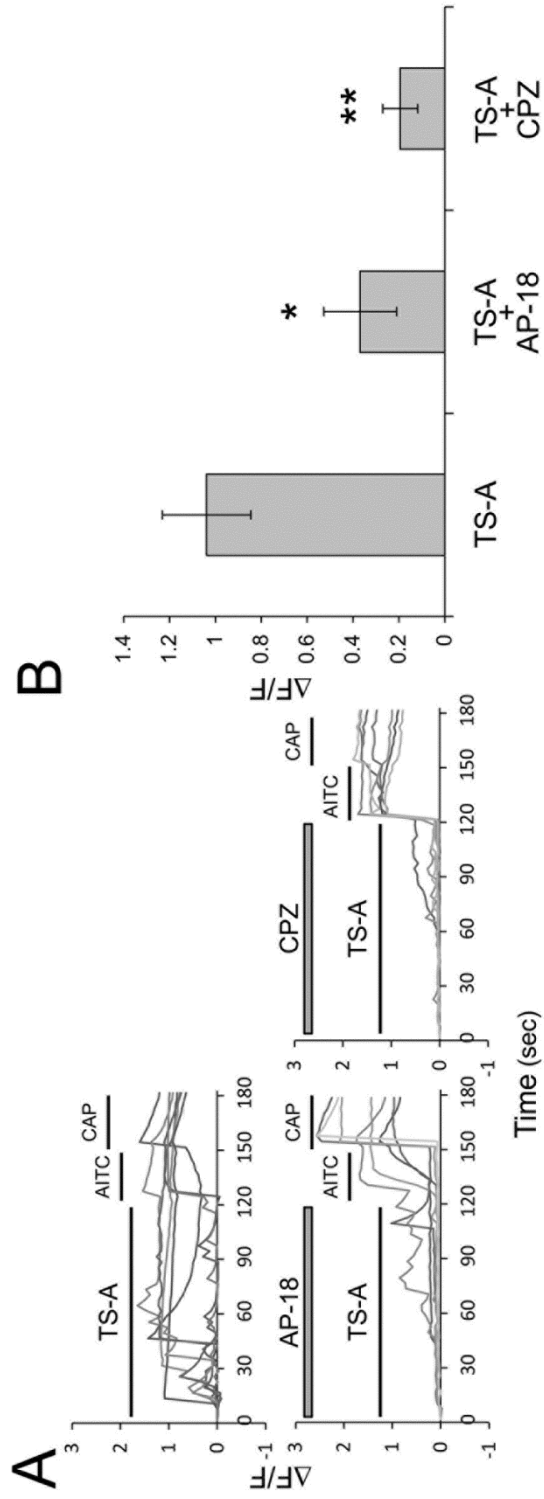
Figure 13
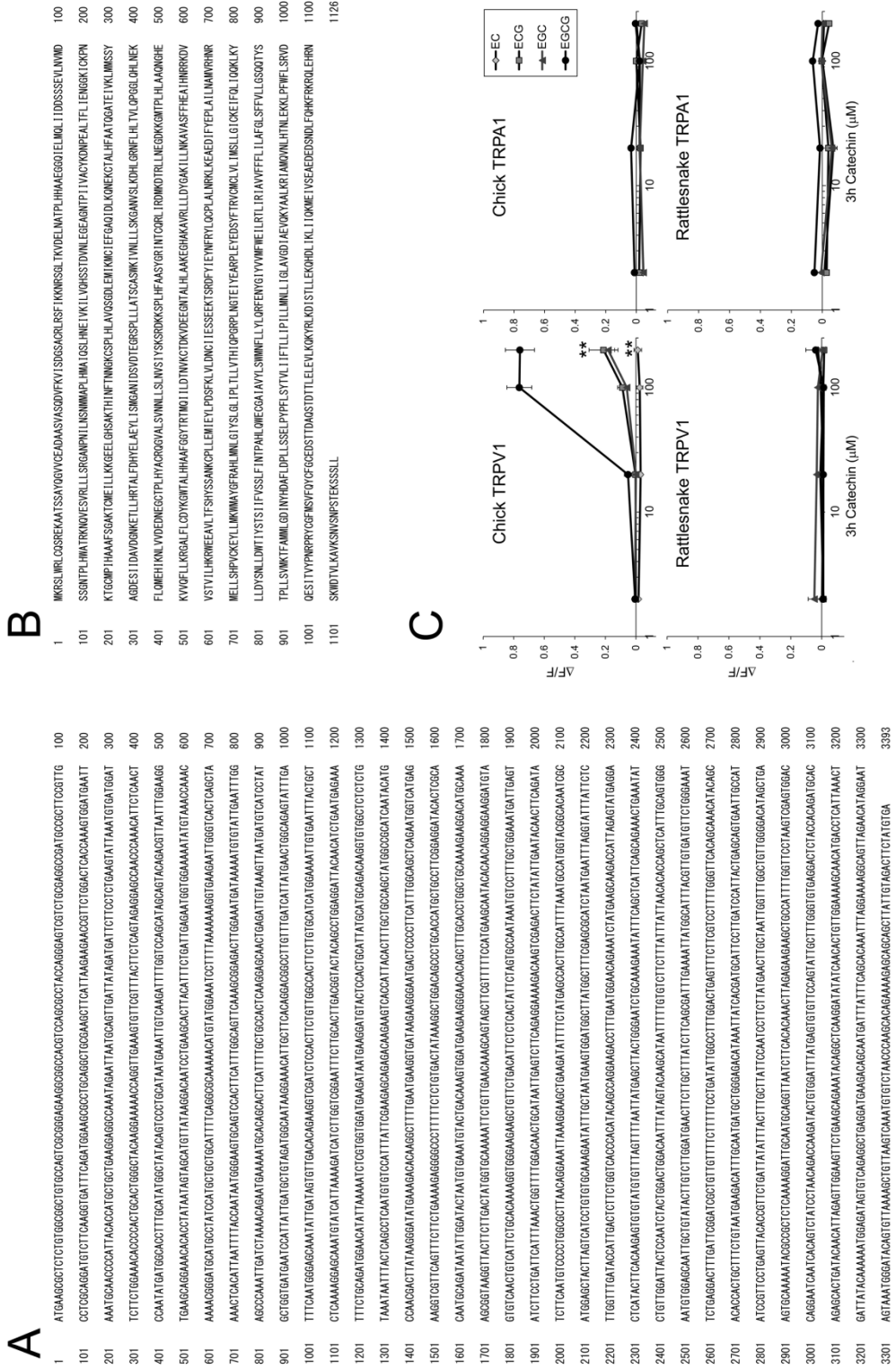
General discussion

In chapterⅠ, I described that intestinal STC-1 cells, which are previously known to respond to five basic taste stimuli, can also respond to the astringent compound of green tea, EGCG, by through activating TRPA1 channels. I further indicated that another TRP channel, TRPV1 can be activated with EGCG. In chapterⅡ, I showed that the freshly prepared EGCG cannot activate TRPV1 and TRPA1 channels but that the incubated and oxidized EGCG can activate these channels. Then, I identified TS-A as a real ligand present in the incubated and oxidized EGCG. Finally, I demonstrated that TS-A can directly activate TRPV1 and TRPA1 channels in DRG sensory neurons isolated from mouse. These studies strongly suggested that the sense of astringency with green tea may be caused by activating TRPV1 and TRPA1 channels with the oxidized catechins such as TS-A in sensory neurons in the tongue and the mouth.

To further prove this my notion about the astringent taste, behavioral analysis of the preference of KO mouse and physiological analysis of its sensory neurons might be useful. TRPV1-KO mouse (Caterina et al., 2000) and TRPA1-KO mouse (Bautista et al., 2006) have been established. But, I have to utilize the TRPV1 and TRPA1-doubly KO mouse, since the astringent compound activates both channels. Further, it is reported that a bitter taste receptor, hTAS2R39 responds to EGCG (Narukawa et al., 2011). Therefore, at least, to investigate the preference behavior of mouse, I have to generate and analyze TAS2R139 (mouse homologue of hTAS2R39)-KO mouse and TRPV1, TRPA1 and TAS2R139-triply KO mouse. The behavioral analysis of the preference using KO mouse is my future work to do.

In this work, I demonstrated one theory that astringency of green tea catechin is caused by activation of TRPV1 and TRPA1 cannels in sensory neurons of tongues. It has been known that nerve fibers in the tongue express TRPV1 (Ishida et al., 2002), and it also

has been shown that TRPA1-positive nerve fibers are present in the tongue (Nagatomo and Kubo, 2008). Primary, sensory neurons are clustered in the dorsal root ganglion (DRG) and within cranial nerve ganglions such as the trigeminal ganglion (TG). It has been reported that DRG and TG neurons express TRPV1, TRPA1, and TRPM8 (Kobayashi et al., 2005). Here, I investigated the sensitivity to the incubated EGCG and TS-A of dissociated sensory neurons in DRG analogous to TG, and I observed a significant activation of neurons though TRP channels. Therefore, it is strongly suggested that both TRPV1 and TRPA1 channels in the nerves innervating the tongue are involved in the perception of the astringency of green tea.

Previously, psychophysical study on astringency supported the notion that astringency is primarily a tactile sensation rather than a taste (Breslin et al., 1993). The mechanism of astringency is not fully understood, although it is known that polyphenols bind and precipitate a class of salivary proteins called the proline-rich proteins (PRPs) (Baxter et al., 1997). One theory is that the precipitation of PRPs from saliva reduces its ability to lubricate, and this loss of lubricity is perceived as an increase in oral friction (Clifford, 1997). A second theory proposes that the sensation is caused by a direct effect of astringents on the oral epithelium and that PRPs play a protective role and prevent astringency by binding the astringent compounds before they can interact with the oral mucosa (Horne et al., 2002). Both theories predict that people with high salivary flow rates and protein/PRP concentrations will report lower ratings of astringency. Several studies support this prediction (Horne et al., 2002; Fischer et al., 1994; Imm et al., 1996; Kallithraka et al., 2001). We propose that astringent compounds, the auto- oxidized catechin and TS-A, activate TRP channels on the sensory nerve endings in the tongue, and that PRPs may play inhibitory role in the sensation of astringency by interacting with these compounds. In addition to PRP, catechins are known to bind directly to many proteins in

serum and in cells, including fibronectin, fibrinogen, histidine-rich glycoprotein, fatty acid synthase, serum albumin, and the laminin receptor (Sazuka et al., 1996; Hayakawa et al., 2001; Bae et al., 2009; Fujimura et al., 2008).   Therefore, it is easily considered that catechins and the oxidized catechins may bind to many kinds of cultured cells.   However, such non-specific binding of catechins cannot induce a significant cellular signaling to lead the activation of sensory neurons.   Namely, for example, normal 3T3 and HEK293T cells were treated with the oxidized products of EGCG, a major tea catechin, no intracellular Ca^{2+} elevation was observed.   But, when mouse TRPA1 or rat TRPV1 was expressed in HEK293T cells and the cells were treated with the oxidized EGCG, a significant Ca^{2+} elevation was induced.   Further, the oxidized EGCG could not activate rat TRPM8 expressed in HEK293T cells.   Thus, specific TRP channels are selectively stimulated with the oxidized EGCG.   Furthermore, the effective concentration of the oxidized EGCG to activate TRPA1 was starting from 100 μM, and to activate TRPV1, only 20 μM of the oxidized EGCG was needed.   AITC, a known specific ligand for TRPA1 is usually used to activate TRPA1 at 100 μM (Maher, et al., 2008).   Capsaicin, a known specific ligand for TRPV1 is usually used to activate TRPV1 at 10 μM (Hellwig et al., 2004).   Observations strongly suggest that activation of TRPA1 and TRPV1 by the oxidized-EGCG must be caused by the specific interaction between TRP channels and the oxidized-EGCG.

Humans have taste buds on the tongue and in the mouth which contain taste receptors. This allows us to sense the basic tastes: sweet, sour, salty, bitter and umami. Smell and chemesthetic also plays a large factor in the flavor of foods.   Volatiles are picked up by the olfactory receptors and in combination with the taste in the mouth, flavor is detected. Without these senses food would lack taste or would have an alteration in the taste perceived (McWilliams et al., 2008).   The taste disorder often comes from diseases such as a cancer, brain tumor or diabetes.   Dysgeusia, or the change in the sense of taste, is a

common side effect of disease as well as disease treatments such as chemotherapy and radiation therapy. Chemotherapy as well as radiation may cause damage to sensory receptors causing dysgeusia or even ageusia which is the complete loss of taste (Rehwaldt et al., 2009). These therapies most specifically abnormality of astringency that can be felt in the sensory nerve, considered that affected by (such as facial nerve paralysis from diabetes) nerve damage. In addition, fungal infections such as thrush, ulcers and dry mouth or xerostoma can also lead to complaints related to dysgeusia (Schiffman, 2007). Some vitamin deficiencies such as zinc, vitamin A and niacin can be related to an altered taste as well (Rehwaldt et al., 2009). Thus, the chemical senses of taste are susceptible to dysfunction. The unfortunate result of dysgeusia and ageusia in the patient leads to a significant downfall in the nutritional status. In future, when we can establish the mechanisms for the taste receptor system of the basic tastes and for the oral chemical senses such as pungent and astringent tastes, details of the cause of the taste disorders will be solved and the suitable medical treatments will be developed.

Molecular Structures
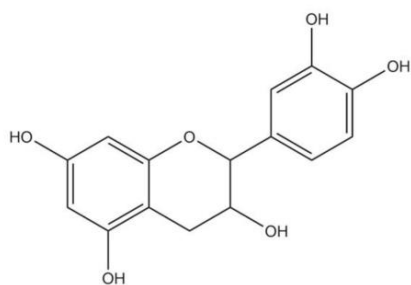
Epicatechin

(EC: MW 290.27)
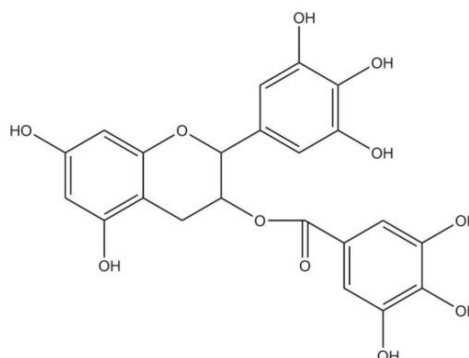
Epicatechin Gallate

(ECG : MW 442.37)
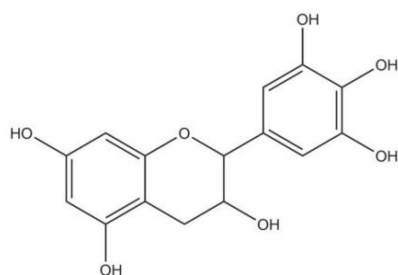
Epigallocatechin
(EGC : MW 306.27)
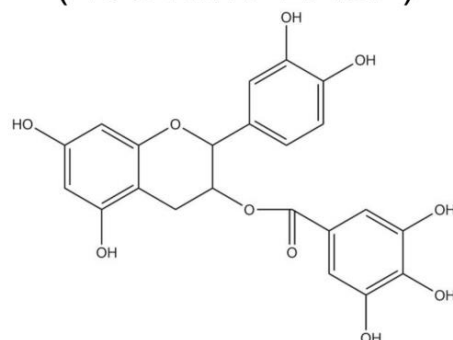
Epigallocatechin Gallate
(EGCG : MW458.37)
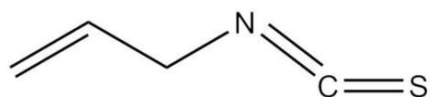
Allyl isothiocyanate
(AITC: MW 99.15)
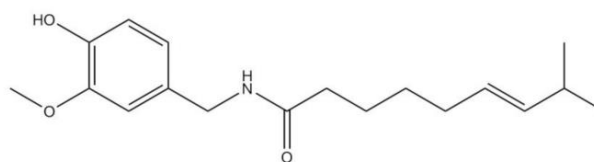
capsaicin (MW 305.41)
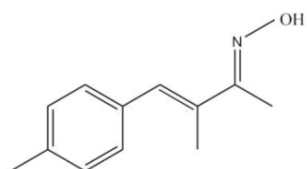
AP18 (MW 209.7)
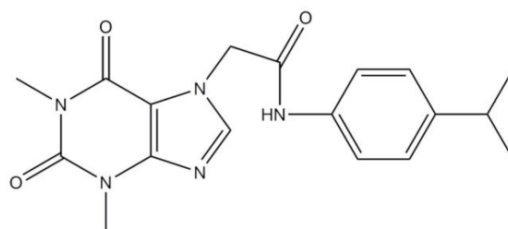
HC030031(MW 355.39)
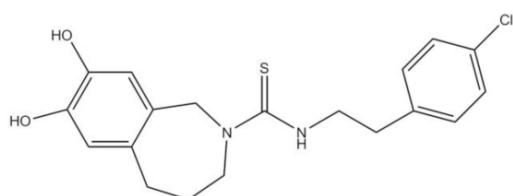
Capsazepin (MW 376.90)
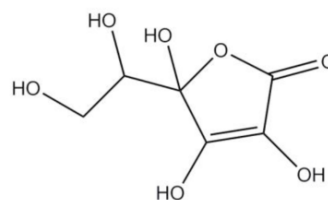
ascorbic acid
(AA: MW 176.13)
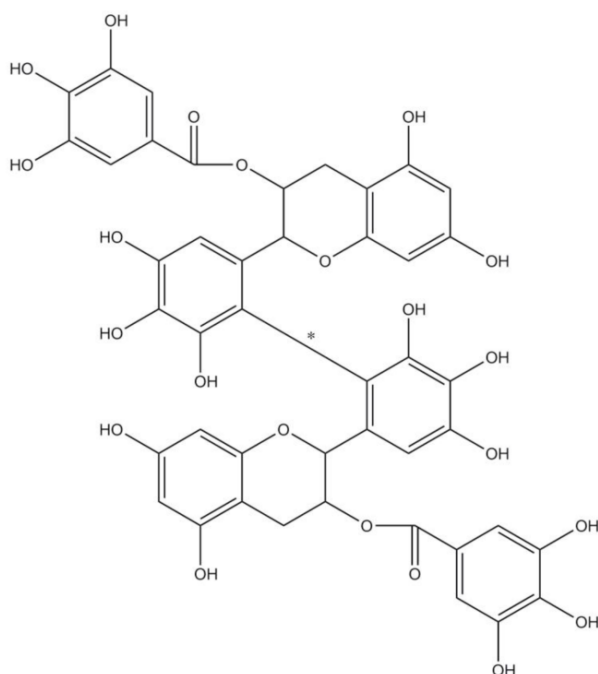
Theasinensin A (TS-A :∗=R)
Theasinensin D (TS-D:∗=S)
(MW: 914.72)

References

Akopian AN, Ruparel NB, Jeske NA, Hargreaves KM. 2007. Transient receptor potential TRPA1 channel desensitization in sensory neurons is agonist dependent and regulated by TRPV1-directed internalization. J Physiol. 583: 175-193.

Akopian AN, Ruparel NB, Patwardhan A, Hargreaves KM. 2008. Cannabinoids desensitize capsaicin and mustard oil responses in sensory neurons via TRPA1 activation. J Neurosci. 28: 1064-1075.

Andersson DA, Gentry C, Moss S, Bevan S. 2008. Transient receptor potential A1 is a sensory receptor for multiple products of oxidative stress. J Neurosci. 28: 2485-2494.

Bae MJ, Ishii T, Minoda K, Kawada Y, Ichikawa T, Mori T, Kamihira M, Nakayama T. 2009. Albumin stabilizes (-)-epigallocatechin gallate in human serum: binding capacity and antioxidant property. Mol Nutr Food Res. 53(6):709-715

Bandell M, Story GM, Hwang SW, Viswanath V, Eid SR, Petrus MJ, Earley TJ, Patapoutian A. 2004. Noxious cold ion channel TRPA1 is activated by pungent compounds and bradykinin. Neuron. 41: 849-857.

Bautista DM, Jordt SE, Nikai T, Tsuruda PR, Read AJ, Poblete J, Yamoah EN, Basbaum AI, Julius D. 2006. TRPA1 mediates the inflammatory actions of environmental irritants and proalgesic agents. Cell.   24; 124 (6): 1269-1282.

Bautista DM, Sigal YM, Milstein AD, Garrison JL, Zorn JA, Tsuruda PR, Nicoll RA, Julius D. 2008. Pungent agents from Szechuan peppers excite sensory neurons by inhibiting two-pore potassium channels. Nat Neurosci. 11: 772-779.

Baxter NJ, Lilley TH, Haslam E, Williamson MP. 1997. Multiple interactions between polyphenols and a salivary proline-rich protein repeat result in complexation and

precipitation. Biochemistry. 36 (18): 5566-5577.

Bettuzzi S, Brausi M, Rizzi F, Castagnetti G, Peracchia G, Corti A. 2006. Chemoprevention of human prostate cancer by oral administration of green tea catechins in volunteers with high-grade prostate intraepithelial neoplasia: a preliminary report from a one-year proof-of-principle study. Cancer Res. 66: 1234-1240.

Breslin PAS, Gilmore MM, Beauchamp GK, Green BG. 1993. Psychophysical evidence that oral astringency is a tactile sensation. Chem Senses 18 (4): 405-417.

Caterina MJ, Leffler A, Malmberg AB, Martin WJ, Trafton J, Petersen-Zeitz KR, Koltzenburg M, Basbaum AI, Julius D. 2000. Impaired nociception and pain sensation in mice lacking the capsaicin receptor. Science. 14; 288 (5464): 306-313.

Caterina MJ, Schumacher MA, Tominaga M, Rosen TA, Levine JD, Julius D. 1997. The capsaicin receptor: a heat-activated ion channel in the pain pathway. Nature. 389: 816-824.

Chandrashekar J, Hoon MA, Ryba NJP, Zucker CS. 2006. The receptors and cells for mammalian taste. Nature. 444: 288-294

Chandrashekar J, Mueller KL, Hoon MA, Adler E, Feng L, Guo W, Zuker CS, Ryba NJP. 2000. T2Rs function as bitter taste receptors. Cell. 100: 703-711.

Chen J, Lake MR, Sabet RS, Niforatos W, Pratt SD, Cassar SC, Xu J, Gopalakrishman S, Pereda-Lopez A, Gopalakrishman M, Holzman TF, Moreland RB, Walter KA, Faltynek CR, Warrior U, Scott VE. 2007. Utility of large-scale transiently transfected cells for cell-based high-throughput screens to identify transient receptor potential channel A1 (TRPA1) antagonist. J Biomol Screen. 12: 61- 69.

Chen MC, Wu SV, Reeve JRJr, Rozengurt E. 2006. Bitter stimuli induce Ca^{2+} signaling and

CCK release in enteroendocrine STC-1 cells: role of L-type voltage-sensitive Ca^{2+} channels. Am J Physiol Cell Physiol. 291: C726-C739.

Chrzanowska-Wodnicka M, Burridge K. 1996. Rho-stimulated contractility drives the formation of stress fibers and focal adhesions. J Cell Biol. 133 (6): 1403-1415.

Chuang HH and Lin S. 2009. Oxidative challenges sensitize the capsaicin receptor by covalent cysteine modification. Proc Natl Acad Sci USA. 106: 20097-20102.

Chung JY, Huang C, Meng X, Dong Z, Yang CS. 1999. Inhibition of activator protein1 activity and cell growth by purified green tea and black tea polyphenols in H-ras-transformed cells: structure-activity relationship and mechanisms involved. Cancer Res. 59: 4610-4617

Citi S and Kendric-Jones J. 1987. Regulation of non-muscle myosin structure and function. Bioessays. 7: 155-159.

Clifford MN. 1997. Astringency. Proceedings of the Phytochemical Society of Europe 41 (Phytochemistry of Fruit and Vegetables): 87-107.

Dai Y, Wang S, Tominaga M, Yamamoto S, Fukuoka T, Higashi T, Kobayashi K, Obata K, Yamanaka H, Noguchi K. 2007. Sensitization of TRPA1 by PAR2 contributes to the sensation of inflammatory pain. J Clin Invest. 117: 1979-1987.

Dockray GJ. 2003. Luminal sensing in the gut: an overview. J Physiol Pharmacol. 54: 9-17.

Drewnowski A and Gomez-Carneros C. 2000. Bitter taste, phytonutrients, and the consumer. Am J Clin Nutr. 72: 1424-1435.

Dyer J, Salmon KSH, Zibrik L, Shirazi-Beechey SP. 2005. Expression of sweet taste receptors of the T1R family in the intestinal tract and enteroendocrine cells. Biochem Soc Trans. 33: 302-305.

Fischer U, Boulton R.B, Noble AC. 1994. Physiological factors contributing to the variability of sensory assessments: relationship between salivary flow rate and temporal perception of gustatory stimuli. Food Quality & Preference 5: 55-64.

Fujimura Y, Umeda D, Kiyohara Y, Sunada Y, Yamada K, Tachibana H. 2006. The involvement of the 67 kDa laminin receptor-mediated modulation of cytoskeleton in the degranulation inhibition induced by epigallocatechin-3-O-gallate. Biochem Biophys Res Comm. 348: 524-531.

Fujimura Y, Umeda D, Yamada K, Tachibana H. 2008. The impact of the 67kDa laminin receptor on both cell-surface binding and anti-allergic action of tea catechins. Arch Biochem Biophys. 15; 476 (2): 133-138.

Gracheva EO, Ingolia NT, Kelly YM, Cordero-Morales JF, Hollopeter G, Chesler AT, Sánchez EE, Perez JC, Weissman JS, Julius D. 2010. Molecular basis of infrared detection by snakes. Nature. 464: 1006-1011.

Green BG. 1993. Oral astringency: a tactile component of flavor. Acta Psychol 84 (1): 119-125.

Hayakawa S, Saeki K, Sazuka M, Suzuki Y, Shoji Y, Ohta T, Kaji K, Yuo A, Isemura M. 2001. Apoptosis induction by epigallocatechin gallate involves its binding to Fas. Biochem Biophys Res Commun. 3; (5): 1102-1106.

Hellwig N, Plant TD, Janson W, Schäfer M, Schultz G, Schaefer M. 2004. TRPV1 acts as proton channel to induce acidification in nociceptive neurons. J Biol Chem. 13; 279 (33): 34553-24561.

Hong J, Lu H, Meng X, Ryu JH, Hara Y, Yang CS. 2002. Stability, cellular uptake, biotransformation, and efflux of tea polyphenol (-)-epigallocatechin-3-gallate in HT-29

human colon adenocarcinoma cells. Cancer Res. 62: 7241-7246.

Horne J, Hayes J, Lawless HT. 2002. Turbidity as a measure of salivary protein reactions with astringent substances. Chem Senses 27 (7): 653-659.

Hou DX, Masuzaki S, Tanigawa S, Hashimoto F, Chen J, Sogo T, Fujii M. 2010. Oolong tea theasinensins attenuate cyclooxygenase-2 expression in lipopolysaccharide (LPS)-activated mouse macrophages: structure-activity relationship and molecular mechanisms. J Agric Food Chem. 58: 12735-12743.

Hou Z, Sang S, You H, Lee MJ, Hong J, Chin KV, Yang CS. 2005. Mechanism of action of (-)-epigallocatechin-3-gallate: auto-oxidation-dependent inactivation of epidermal growth factor receptor and direct effects on growth inhibition in human esophageal cancer KYSE 150 cells. Cancer Res. 65: 8049-8056.

Huang AL, Chen X, Hoon MA, Chandrashekar J, Guo W, Trankner D, Ryba NJP, Zuker CS. 2006. The cells and logic for mammalian sour taste detection. Nature. 442: 934-938.

Imm B and Lawless HT. 1996. Relationships between salivary responses and astringency, bitterness and sourness responses to aluminum ammonium sulfate. Chem Senses. 21 (5): 618.

Ishida Y, Ugawa S, Ueda T, Murakami S, Shimada S. 2002. Vanilloid receptor subtype-1 (VR1) is specifically localized to taste papillae. Mol Brain Res. 107: 17-22.

Ishimaru Y, Inada H, Kubota M, Zhuang H, Tominaga M, Matsunami H. 2006. Transient receptor potential family members PKD1L3 and PKD2L1 form a candidate sour taste receptor. Proc Natl Acad Sci USA. 103: 12569-12574.

Ishimaru Y. 2009. Molecular mechanism of taste transduction in vertebrates. Odontology. 97: 1-7.

Jordt SE and Julius D. 2002. Molecular basis for species-specific sensitivity to "hot" chili peppers. Cell. 108: 421-430.

Jordt SE, Bautista DM, Chuang HH, McKemy DD, Zygmunt PM, Högestätt ED, Meng ID, Julius D. 2004. Mustard oils and cannabinoids excite sensory nerve fibres through the TRP channel ANKTM1. Nature. 427: 260-265.

Kallithraka S, Bakker J, Clifford MN, Vallis L. 2001. Correlations between saliva protein composition and some T-I parameters of astringency. Food Quality & Preference 12 (2): 145-152.

Karashima Y, Damann N, Prenen J, Talavera K, Segal A, Voets T, Nilius B. 2007. Bimodal Action of Menthol on the Transient Receptor Potential Channel TRPA1. J Neurosci. 27: 9874-9884.

Kerstein PC, Camino Dd, Moran MM, Stucky1 CL. 2009. Pharmacological blockade of TRPA1 inhibits mechanical firing in nociceptors. Mol Pain. 5: 19.

Kobayashi K, Fukuoka T, Obata K, Yamanaka H, Dai Y, Tokunaga A, Noguchi K. 2005. Distinct expression of TRPM8, TRPA1, and TRPV1 mRNAs in rat primary afferent neurons with adelta/c-fibers and colocalization with trk receptors. J Comp Neurol. 493: 596-606.

Kurogi M, Miyashita M, Emoto Y, Kubo Y, Saitoh O. 2012. Green tea polyphenol epigallocatechin gallate activates TRPA1 in an intestinal enteroendocrine cell line, STC-1. Chem Senses. 37: 167-177.

Lesschaeve I and Nobel AC. 2005. Polyphenols: factors influencing their sensory properties and their effects on food and beverage preferences. Am J Clin Nutr. 81: 330S-335S.

Macpherson LJ, Geierstanger BH, Viswanath V, Bandell M, Eid SR, Hwang S, Patapoutian

A. 2005. The pungency of garlic: activation of TRPA1 and TRPV1 in response to allicin. Curr Biol. 15: 929-934.

Maher M, Ao H, Banke T, Nasser N, Wu NT, Breitenbucher JG, Chaplan SR, Wickenden AD. 2008. Activation of TRPA1 by farnesyl thiosalicylic acid. Mol Pharm 73: 1225-1234.

Margolskee RF, Dyer J, Kokrashvili Z, Salmon KS, Ilegems E, Daly K, Maillet EL, Ninomiya Y, Mosinger B, Shirazi-Beechey SP. 2007. T1R3 and gustducin in gut sense sugars to regulate expression of Na^+-glucose cotransporter 1. Proc Natl Acad Sci USA. 104: 15075-15080.

Masuho I, Tateyama M, Saitoh O. 2005. Characterization of bitter taste responses of intestinal STC-1 cells. Chem Senses. 30: 281-290.

McNamara CR, Mandel-Brehm J, Bautista DM, Siemens J, Deranian KL, Zhao M, Hayward NJ, Chong JA, Julius D, Moran MM, Fanger CM. 2007. TRPA1 mediates formalin-induced pain. Proc Natl Acad Sci USA. 104: 13525-13530.

McWilliams, M. 2008. Foods: experimental perspectives. 6th ed. Ohio: Pearson Prentice Hall. 45-52.

Mehansho H, Butler LG, Carlson DM. 1987. Dietary tannins and salivary proline-rich proteins: interactions, induction, and defense mechanisms. Annu Rev Nutr. 7: 423-440.

Murray NJ, Williamson MP, Lilley TH, Haslam E. 1994. Study of the interaction between salivary proline-rich proteins and a polyphenol by 1H-NMR spectroscopy. Eur J Biochem. 1; 219 (3): 923-935.

Nagatomo K and Kubo Y. 2008. Caffeine activates mouse TRPA1 channels but suppresses human TRPA1 channels. Proc Natl Acad Sci USA. 105: 17373-17378.

Narukawa M, Noga C, Ueno Y, Sato T, Misaka T, Watanabe T. 2011. Evaluation of the bitterness of green tea catechins by a cell-based assay with the human bitter taste receptor hTAS2R39. Biochem. Biophys. Res. Comm. 405: 620-625.

Nelson G, Chandrashekar J, Hoon MA, Feng L, Zhao G, Ryba NJP, Zuker CS. 2002. An amino-acid taste receptor. Nature. 416: 199-202.

Nelson G, Hoon MA, Chandrashekar J, Zhang Y, Ryba NJP, Zuker CS. 2001. Mammalian sweet taste receptors. Cell. 106: 381-390.

Oda M, 2013. Molecular characterization of fish TRPA1 channel activation by chemical and thermal stimuli. Thesis for master degree. (Nagahama Institute of Bio-Science and Technology).

Peleg H, Gacon K, Schlich P, Noble CA. 1999. Bitterness and astringency of flavan-3-ol monomers, dimers and trimmers. J Sci Food Agric. 79: 1123-1128.

Petrus P, Peier AM, Bandell M, Hwang SW, Huynh T, Olney N, Jegla T, Patapoutian A. 2007. A role of TRPA1 in mechanical hyperalgesia is revealed by pharmacological inhibition. Mol Pain. 3: 40.

Prober DA, Zimmerman S, Myers BR, McDermott BM Jr, Kim SH, Caron S, Rihel J, Solnica-Krezel L, Julius D, Hudspeth AJ, Schier AF. 2008. J Neurosci. 1; 28 (40): 10102-10110.

Rehwaldt M, Wickman R, Purl S, Tariman J, Blendowski C and others. 2009. Self-care strategies to cope with taste changes after chemotherapy. Oncology Nursing Forum. 36 (2): E47-E56.

Ridley AJ and Hall A. 1992. The small GTP-binding protein rho regulates the assembly of focal adhesions and actin stress fibers in response to growth factors. Cell. 7; 70 (3):

389-399.

Rindi G, Grant SGN, Yiangou Y, Ghatei MA, Bloom SR, Bautch VL, Solcia E, Polak JM. 1990. Development of neuroendocrine tumors in the gastrointestinal tract of transgenic mice. Heterogeneity of hormone expression. Am J Pathol. 136: 1349-1363.

Saeki K, Hayakawa S, Isemura M, Miyase T. 2000. Importance of a pyrogallol- type structure in catechin compounds for apoptosis-inducing activity. Phytochemistry. 53: 391-394.

Saito S, Nakatsuka K, Takahashi K, Fukuta N, Imagawa T, Ohta T, Tominaga M. 2012. Analysis of transient receptor potential ankyrin 1 (TRPA1) in frogs and lizards illuminates both nociceptive heat and chemical sensitivities and coexpression with TRP vanilloid 1 (TRPV1) in ancestral vertebrates. J Biol Chem. 287: 30743-30754.

Saitoh O, Hirano A, Nishimura Y. 2007. Intestinal STC-1 cells respond to five basic taste stimuli. Neuroreport. 18: 1991-1995.

Sang S, Lee MJ, Hou Z, Ho CT, Yang CS. 2005. Stability of tea polyphenol (-)- epigallocatechin-3-gallate and formation of dimers and epimers under common experimental conditions. J Agric Food Chem. 53: 9478-9484.

Sawada Y, Hosokawa H, Matsumura K, Kobayashi S. 2008. Activation of transient receptor potential ankyrin 1 by hydrogen peroxide. Eur J Neurosci. 27: 1131-1142.

Sazuka M, Itoi T, Suzuki Y, Odani S, Koide T, Isemura M. 1996. Evidence for the interaction between (-)-epigallocatechin gallate and human plasma proteins fibronectin, fibrinogen, and histidine-rich glycoprotein. Biosci Biotechnol Biochem. 60 (8): 1317-1319.

Schiffman SS, Suggs MS, Simon SA. Astringent compounds suppress taste responses in

gerbil. Brain Res. 6; 595 (1): 1-11.

Schiffman SS. 2007. Critical illness and changes in sensory perception. Proceedings of the Nutrition Society. 66: 331-345.

Shii T, Miyamoto M, Matsuo Y, Tanaka T, Kouno I. 2011. Biomimetic one-pot preparation of a black tea polyphenol theasinensin A from epigallocatechin gallate by treatment with copper(II) chloride and ascorbic acid. Chem Pharm Bull. 59: 1183-1185.

Slack JP, Brockhoff A, Batram C, Menzel S, Sonnabend C, Born S, Galindo MM, Kohl S, Thalmann S, Ostopovici-Halip L, Simons CT, Ungureanu I, Duineveld K, Bologa CG, Behrens M, Furrer S, Oprea TI, Meyerhof W. 2010. Modulation of bitter taste perception by a small molecule hTAS2R antagonist. Curr Biol. 22; 20 (12): 1104-1109.

Staruschenko A, Jeske NA, Akopian AN. 2010. Contribution of TRPV1-TRPA1 interaction to the single channel properties of the TRPA1 channel. J Biol Chem. 285: 15167-15177.

Tachibana H, Koga K, Fujimura Y, Yamada K. 2004. A receptor for green tea polyphenol EGCG. Nat Struc Mol Biol. 11: 380-381.

Takahashi N, Mizuno Y, Kozai D, Yamamoto S, Kiyonaka S, Shibata T, Uchida K, Mori Y. 2008. Molecular characterization of TRPA1 channel activation by cysteine-reactive inflammatory mediators. Channels (Austin). 2: 287-298.

Umeda D, Tachibana H, Yamada K. 2005. Epigallocatechin-3-O-gallate disrupts stress fibers and the contractile ring by reducing myosin regulatory light chain phosphorylation mediated through the target molecule 67 kDa laminin receptor. Biochem Biophys Res Commun. 333: 628-635.

Umeda D, Yano S, Yamada K, Tachibana H. 2008. Green tea polyphenol epigallocatechin-3-gallate signaling pathway through 67-kDa laminin receptor. J Biol

Chem. 283: 3050-3058.

Wang Z-Y, Huang M-T, Ferraro T, Wong C-Q, Lou Y- R, Reuhl K, Iatropoulos M, Yang CS, Conney AH. 1992. Inhibitory effect of green tea in the drinking water on tumorigenesis by ultraviolet light and 12-O-tetradecanoylphorbol-13-acetate in the skin of SKH-1 mice. Cancer Res. 52: 1162-1170.

Wolfram S. 2007. Effetcs of green tea and EGCG on cardiovascular and metabolic health. J Am Coll Nutr. 26: 373S-388S.

Wu SV, Rozengurt N, Yang M, Young SH, Sinnett-Smith J, Rozengurt E. 2002. Expression of bitter taste receptors of the T2R family in the gastrointestinal tract and enteroendocrine STC-1 cells. Proc Natl Acad Sci USA. 99: 2392-2397.

Yang CS, Sang S, Lambert JD, Hou Z, Ju J, Lu G. 2006. Possible mechanisms of the cancer-preventive activities of green tea. Mol Nutr Food Res. 50: 170-175.

Acknowledgements